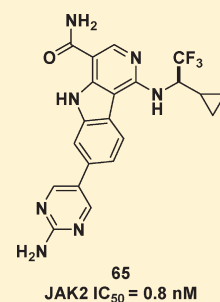


Discovery of 1-Amino-5*H*-pyrido[4,3-*b*]indol-4-carboxamide Inhibitors of Janus Kinase 2 (JAK2) for the Treatment of Myeloproliferative Disorders<sup>†</sup>Jongwon Lim,<sup>\*,†</sup> Brandon Taoka,<sup>‡</sup> Ryan D. Otte,<sup>‡</sup> Kerrie Spencer,<sup>‡</sup> Christopher J. Dinsmore,<sup>‡</sup> Michael D. Altman,<sup>‡</sup> Grace Chan,<sup>||</sup> Craig Rosenstein,<sup>||</sup> Sujata Sharma,<sup>∞</sup> Hua-Poo Su,<sup>∞</sup> Alexander A. Szewczak,<sup>||</sup> Lin Xu,<sup>#</sup> Hong Yin,<sup>#</sup> Joan Zugay-Murphy,<sup>∞</sup> C. Gary Marshall,<sup>§</sup> and Jonathan R. Young<sup>‡</sup>Departments of <sup>†</sup>Chemistry, <sup>§</sup>Oncology, <sup>||</sup>In Vitro Pharmacology, <sup>‡</sup>Chemistry Modeling and Informatics, <sup>#</sup>Drug Metabolism and Pharmacokinetics, and <sup>∞</sup>Structural Chemistry, Merck & Co., Inc., 33 Avenue Louis Pasteur, Boston, Massachusetts 02115, United States

## Supporting Information

**ABSTRACT:** The JAK-STAT pathway mediates signaling by cytokines, which control survival, proliferation, and differentiation of a variety of cells. In recent years, a single point mutation (V617F) in the tyrosine kinase JAK2 was found to be present with a high incidence in myeloproliferative disorders (MPDs). This mutation led to hyperactivation of JAK2, cytokine-independent signaling, and subsequent activation of downstream signaling networks. The genetic, biological, and physiological evidence suggests that JAK2 inhibitors could be effective in treating MPDs. De novo design efforts of new scaffolds identified 1-amino-5*H*-pyrido[4,3-*b*]indol-4-carboxamides as a new viable lead series. Subsequent optimization of cell potency, metabolic stability, and off-target activities of the leads led to the discovery of 7-(2-aminopyrimidin-5-yl)-1-[(1*R*)-1-cyclopropyl-2,2,2-trifluoroethyl]amino}-5*H*-pyrido[4,3-*b*]indole-4-carboxamide (**65**). Compound **65** is a potent, orally active inhibitor of JAK2 with excellent selectivity, PK profile, and in vivo efficacy in animal models.



## INTRODUCTION

Janus kinase 2 (JAK2) is an intracellular nonreceptor tyrosine kinase that belongs to the JAK family kinases (JAK1, JAK2, JAK3, and TYK2). The JAK-signal transducer and activator of transcription (JAK-STAT) pathway mediates signaling by cytokines, which control survival, proliferation, and differentiation of a variety of cells.<sup>1–4</sup> JAK2 signals downstream of a variety of cytokine receptors, including receptors for interleukin-3 (IL-3), granulocyte-macrophage colony stimulating factor (GM-CSF), erythropoietin (EPO), and thrombopoietin (TPO).<sup>5</sup> Cytokine binding results in JAK2 phosphorylation, downstream STAT phosphorylation (usually STAT3 and STAT5), and activation of gene transcription. For all of these cytokines, activation of this signaling cascade ultimately results in increased proliferation, differentiation, and survival of erythroid and myeloid cells, and JAK2 plays a key role in the maintenance of balanced hematopoiesis in adult tissues.

In 2005, several groups independently reported the discovery of a somatic mutation of the gene encoding JAK2 in a high proportion of patients with myeloproliferative disorders (MPDs): >95% for polycythemia vera (PV) and 50% for essential thrombocythemia (ET) and primary myelofibrosis (PMF).<sup>6–10</sup> A single valine to phenylalanine mutation at position 617, located in the pseudokinase domain thought to negatively regulate the adjacent kinase domain, results in increased JAK2 autophosphorylation and subsequent activation of downstream signaling networks. The JAK2<sup>V617F</sup> mutation of JAK2 confers cytokine-independent proliferation and survival of a previously EPO-dependent cell line,

consistent with its role in mediating EPO signaling. Remarkably, reconstitution of irradiated mice with transduced bone marrow expressing JAK2<sup>V617F</sup> leads to a condition that strongly resembles PV within 4–6 weeks, with overt erythrocytosis, splenomegaly, and in some strains of mice, leukocytosis.<sup>11–13</sup> Thus, there is genetic, cell based, and in vivo evidence to suggest a functional role for mutant JAK2 in the pathology of PV, and it is reasonable to predict that targeting the JAK2 protein could have therapeutic benefit in this patient population. In fact, several classes of JAK2 inhibitors have been developed and are being tested in clinical trials for the treatment of MPDs.<sup>14</sup> The purpose of this report is to describe the discovery of a series of novel small molecule inhibitors of JAK2 that could reverse hyperphosphorylation of JAK2 and be effective in treating MPD patients.

In 2002, researchers at Merck reported discovery of 1,6-dihydro-7*H*-benzo[*h*]imidazo[4,5-*f*]isoquinolin-7-ones as potent JAK inhibitors.<sup>15–17</sup> These novel tetracyclics are generally pan-JAK family inhibitors (IC<sub>50</sub> for **1** in Figure 1: JAK1 = 2 nM, JAK2 = 3 nM, JAK3 = 77 nM, and TYK2 = 7 nM) and have high selectivity against other kinases. Recently, these laboratories reported that compound **1** prevented EPO-induced PV in mice with lower hematocrits, reduced spleen sizes, and reductions in pSTAT5.<sup>18</sup> Although **1** showed good efficacy in the in vivo model and displayed desirable pharmacokinetic (PK) properties in rats (see Table 1), suboptimal physical properties and the poor kinase

Received: July 11, 2011

Published: September 26, 2011

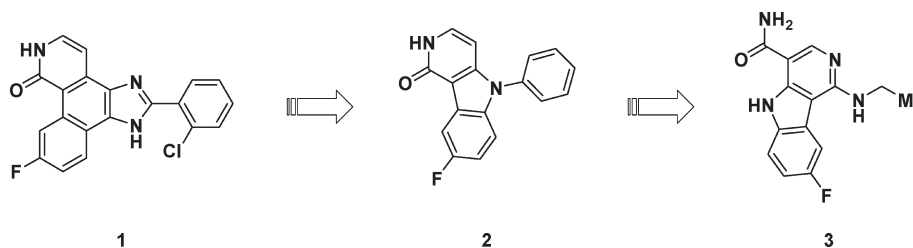


**Figure 1.** De novo design of the 1-amino-5H-pyrido[4,3-*b*]indol-4-carboxamide core.

**Table 1.** Key Comparisons of Compounds 1–3

|                                    | 1                | 2               | 3                              |
|------------------------------------|------------------|-----------------|--------------------------------|
| JAK2 IC <sub>50</sub> (nM)         | 3                | 1,100           | 230                            |
| JAK3 IC <sub>50</sub> (nM)         | 77               | 720             | 6,800                          |
| JAK3/JAK2 IC <sub>50</sub> (ratio) | 26               | 0.7             | 30                             |
| rat PK properties                  |                  |                 |                                |
| Cl <sub>p</sub> (mL/min/kg)        | 5.4 <sup>a</sup> | 13 <sup>b</sup> | >Q <sub>hep</sub> <sup>c</sup> |
| bioavailability (%)                | 100 <sup>a</sup> | 89 <sup>b</sup> | 87 <sup>c</sup>                |
| physical properties                |                  |                 |                                |
| log <i>D</i> (pH 7.4)              | 3.6              | 4.3             | 2.0                            |
| aqueous solubility (μM)            | <2               | 0               | 6                              |

<sup>a</sup> iv at 2 mg/kg, po at 4 mg/kg; dosed as a solution in DMSO/PEG400/water (30:30:40). <sup>b</sup> iv at 1 mg/kg, po at 2 mg/kg; dosed as a solution in PEG400/water (50:50). <sup>c</sup> iv at 1 mg/kg, po at 2 mg/kg; dosed as a solution in PEG400/40% Captisol (50:50); Q<sub>hep</sub> = hepatic blood flow.

selectivity profile within the JAK family in this series hampered further lead optimization efforts.

De novo design of new scaffolds derived from **1** was pursued to rapidly identify a new viable lead series. Efforts to improve physical properties embedded in the tetracyclic core led to the identification of a tricyclic core, 2,5-dihydro-1H-pyrido[4,3-*b*]indol-1-one (**2**), which maintained key pharmacophores including the two-point hinge binding motif of the pyridone. Although **2** presented promising PK properties in rats, this series was abandoned because of moderate JAK2 potency of the analogues, poor selectivity over JAK3, and poor physical properties. A structurally related class was subsequently identified from the IκB kinase (IKK) program within Merck<sup>19</sup> and tested in a focused screen format prior to the high throughput screening campaign of the Merck compound collection. This led to the identification of 1-amino-5H-pyrido[4,3-*b*]indol-4-carboxamides exemplified by compound **3** (Figure 1) as a new lead series. Compared to **2**, compound **3** not only has an improved potency and selectivity over JAK3 but also possesses much more druglike physical properties including log *D* and aqueous solubility. Additional in vitro profiling indicated that **3** was an ATP competitive inhibitor of JAK2 based on a stark potency shift at a higher ATP concentration (IC<sub>50</sub> = 230 nM at 15 μM ATP; IC<sub>50</sub> > 15 000 nM at 2 mM ATP). Molecular modeling attributed this to a three-point binding interaction of the amide and the indole nitrogen to the hinge region of the JAK2 protein.

Herein, we report a series of modifications to the amine and the C-ring moieties of the 1-amino-5H-pyrido[4,3-*b*]indol-4-carboxamide core of **3**. Sequential improvements in cell potency, metabolic profile, hERG activity,<sup>20</sup> and P450 inhibitory activities led to the discovery of 7-(2-aminopyrimidin-5-yl)-1-[(1*R*)-1-cyclopropyl-2,2,2-trifluoroethyl]amino}-5H-pyrido[4,3-*b*]indole-4-carboxamide (**65**), a

potent, selective, and orally active JAK2 inhibitor with an excellent PK profile in three preclinical species. In addition, initial in vivo efficacy results of **65** in PV mouse models are described.

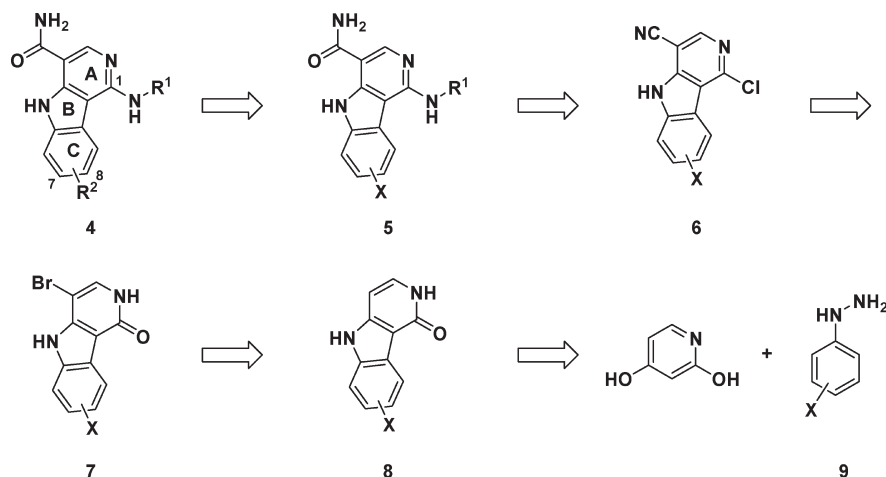
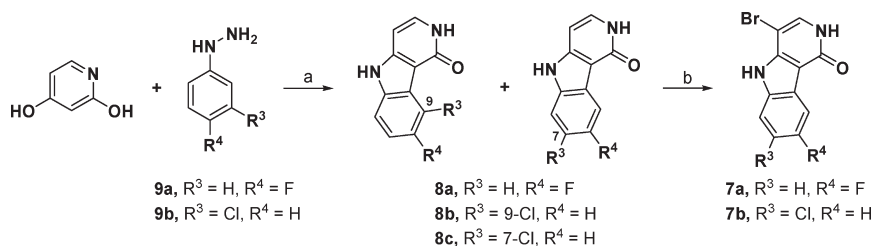
## CHEMISTRY

A general retrosynthetic analysis toward the 1-amino-5H-pyrido[4,3-*b*]indol-4-carboxamide core (**4**) is outlined in Scheme 1. Substituents on the C-ring were introduced via palladium mediated coupling conditions from intermediates **5** (X = Cl).<sup>21,22</sup> Amines were coupled to the chloropyridine moiety of A-ring, which was prepared from the pyridone employing POCl<sub>3</sub>, followed by hydrolysis of the nitrile to the primary amide group. The nitrile was installed through a sequential NBS bromination and Negishi coupling<sup>23</sup> from the pyridone intermediates **8**. Intermediates **8** were then constructed via Fischer indole synthesis<sup>24</sup> between 2,4-dihydroxypyridine and substituted phenylhydrazines (**9**). The following schemes (Scheme 2–5) provide an overview of the synthetic routes and reaction conditions for representative 1-amino-5H-pyrido[4,3-*b*]indol-4-carboxamides.

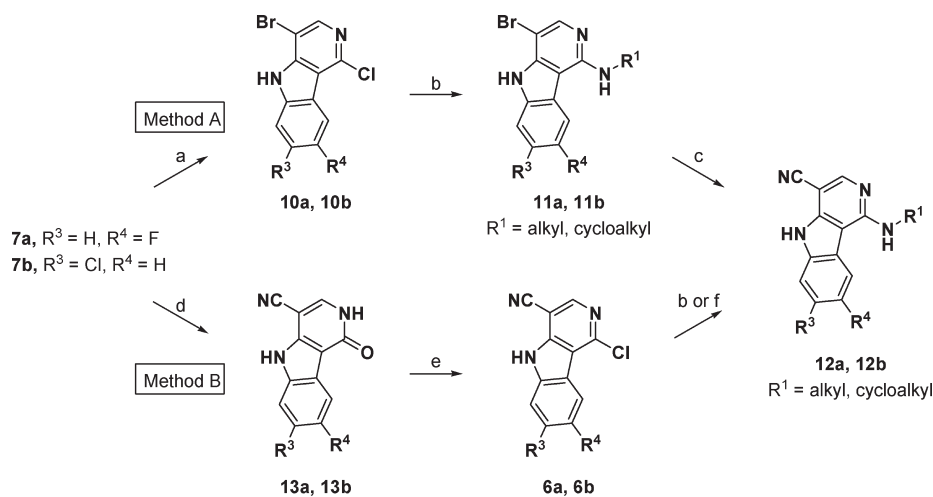
The 2,5-dihydro-1H-pyrido[4,3-*b*]indol-1-one cores were synthesized in one step via condensation between 2,4-dihydroxypyridine and substituted phenylhydrazines with the removal of water (Scheme 2).<sup>24</sup> For 3-chlorophenylhydrazine (**9b**), a mixture of 7- and 9-chloro regioisomers (**8c** and **8b**) was formed in a ratio of 3:2, which could be separated at this stage. Bromination took place at the 4-position of the A-ring selectively, which was useful for further functionalization.

The A-ring of the cores was then derivatized as shown in Scheme 3. Pyridones **7** were converted to chloropyridines **10** with POCl<sub>3</sub>, to which various amines were added to afford aminopyridines **11** (method A in Scheme 3). The nitrile group was then introduced to the 4-position of the cores employing CuCN. Alternatively, intermediates **7** were converted to nitriles **13** via Negishi coupling<sup>23</sup> before the conversion to chloropyridines **6** (method B in Scheme 3). Electron rich amines could be added to intermediates **6** in either thermal or microwave irradiation conditions. However, amines that have fluorine atoms on the β-carbon were not nucleophilic enough and failed to couple to intermediates **6** in these conditions. For those amines, the coupling could be realized via palladium mediated coupling conditions.<sup>25,26</sup> Compared to method A, method B has the diversifying point at a later stage of the synthesis and was employed more frequently for a rapid SAR studies on the C-1 amines.

As shown in Scheme 4, 1-substituted-1-cyclopropylmethanamines were prepared employing Ellman chemistry.<sup>27,28</sup> Cyclopropanecarboxaldehyde was condensed with sulfonamides **13** in the presence of PPTS and magnesium sulfate to form imines **14**.

Scheme 1. Retrosynthetic Analysis toward the 1-Amino-5*H*-pyrido[4,3-*b*]indol-4-carboxamide CoreScheme 2. Construction of the 2,5-Dihydro-1*H*-pyrido[4,3-*b*]indol-1-one Cores<sup>a</sup>

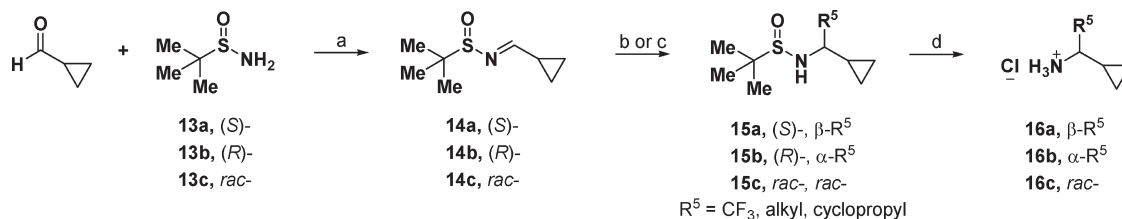
<sup>a</sup> (a) Dean–Stark trap, Ph<sub>2</sub>O, 175–230 °C; (b) NBS, DMF.

Scheme 3. Synthesis of the 1-Amino-5*H*-pyrido[4,3-*b*]indole-4-carbonitriles<sup>a</sup>

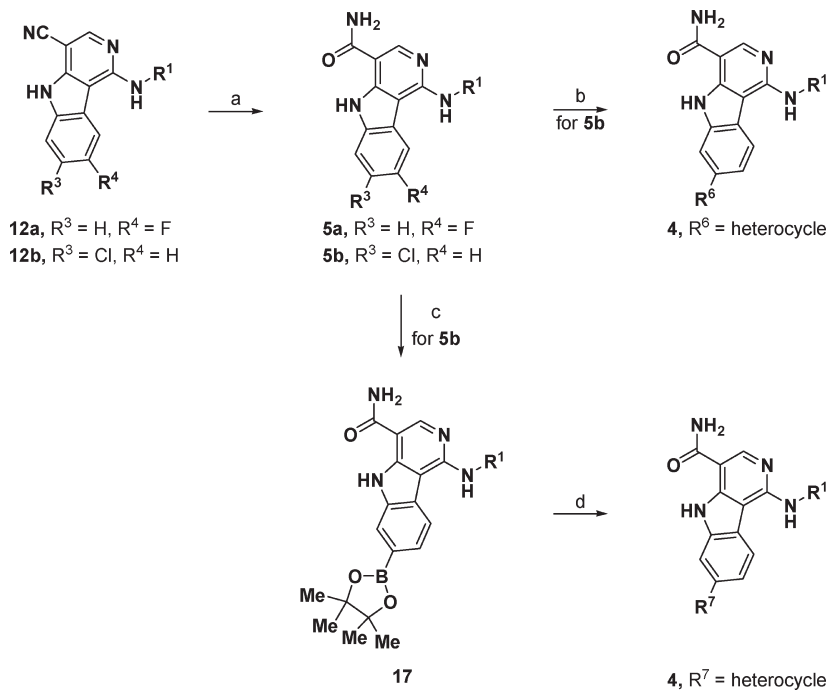
<sup>a</sup> (a) POCl<sub>3</sub>, microwave, 175 °C; (b) amine, MeOH, heat or microwave; (c) CuCN, NMP, microwave, 225 °C; (d) Zn(CN)<sub>2</sub>, Pd(PPh<sub>3</sub>)<sub>4</sub>, DMF, 90 °C; (e) POCl<sub>3</sub>, dioxane, 90 °C; (f) amine, Pd<sub>2</sub>(dba)<sub>3</sub>, BINAP, NaO<sup>t</sup>Bu, DME, 85 °C.

Compounds **14** were then treated with nucleophiles such as CF<sub>3</sub>TMS/TMAF<sup>29</sup> for the introduction of CF<sub>3</sub> group and alkyl Grignard reagents for the introduction of the corresponding alkyl groups to afford **15**. The nucleophilic additions provided high degrees of diastereoselectivity. Moreover, the major

diastereomers could be separated from the minor diastereomers by SiO<sub>2</sub> chromatography at this stage. After the isolation of the diastereomerically pure sulfinamides **15a** and **15b**, the *tert*-butylsulfinyl group was removed with 4 N HCl to provide **16**.

Scheme 4. Synthesis of 1-Substituted-1-cyclopropylmethanamines<sup>a</sup>

<sup>a</sup> (a) MgSO<sub>4</sub>, PPTS, DCM; (b) CF<sub>3</sub>TMS, TMAF, THF, -55 °C; (c) R<sup>5</sup>MgCl or R<sup>5</sup>MgBr, DCM, -78 to -52 °C; (d) 4 N HCl, MeOH/dioxane.

Scheme 5. Functionalization of the C-Ring<sup>a</sup>

<sup>a</sup> (a) Aqueous H<sub>2</sub>O<sub>2</sub>, K<sub>2</sub>CO<sub>3</sub>, DMSO, 70 °C; (b) R<sup>6</sup>-boronic ester, Pd<sub>2</sub>(dba)<sub>3</sub>, PCy<sub>3</sub>, K<sub>3</sub>PO<sub>4</sub>, dioxane/water, 100 °C; (c) bis(pinacolato)diboron, Pd<sub>2</sub>(dba)<sub>3</sub>, PCy<sub>3</sub>, KOAc, dioxane, microwave, 150 °C; (d) R<sup>7</sup>-Cl, Pd<sub>2</sub>(dba)<sub>3</sub>, PCy<sub>3</sub>, K<sub>3</sub>PO<sub>4</sub>, dioxane/water, 100 °C.

Upon completion of the introduction of amines at the 1-position, the nitrile group was hydrolyzed with aqueous H<sub>2</sub>O<sub>2</sub> and K<sub>2</sub>CO<sub>3</sub> at an elevated temperature (**5** in Scheme 5). The C7-Cl group on the C-ring was then derivatized with aryl and heteroaryl boronic esters by employing palladium mediated coupling conditions.<sup>21,22</sup> For heteroaryl chloride or bromide coupling partners, the chloro group on the C-ring was first converted to the corresponding pinacol boronic esters **17** and subsequently coupled to heteroaryl halides to provide the coupled products **4**.

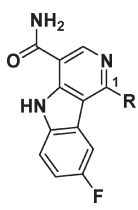
## RESULTS AND DISCUSSIONS

**Initial Substitutions at C-1 of the A-Ring.** Our initial SAR efforts were directed toward varying the amine substituent at the 1-position of the 5H-pyrido[4,3-*b*]indol-4-carboxamide core to improve JAK2 potency (Table 2). To this end, a diverse range of aliphatic amines were investigated. When straight alkylamines were examined, it was found that JAK2 potency improved as the size of the amine increased, as butylamine **20** was 4-fold more potent than either methylamine **18** or ethylamine **3**. Branched alkylamines that have substituents at  $\alpha$ - and  $\beta$ -positions of the

amine gave either comparable or improved JAK2 activities. While isobutylamine **22** showed comparable potency to propylamine **19**, isopropylamine **21** was twice as potent as ethylamine **3**, indicating a preference for an  $\alpha$ -branched amine. The use of  $\alpha$ -branched bulky amine added to C-1 further improved JAK2 potency exemplified by (2*S*)-3,3-dimethylbutan-2-amine **23** (IC<sub>50</sub> = 52 nM). It was also found that stereochemistry of the  $\alpha$ -branch of the amine was important, as **23** was found to be 4-fold more potent than the (*R*)-enantiomer **24**.

Major improvements in JAK2 potency were observed with cycloalkylamines at C-1 position of the core. As was the trend for acyclic alkylamines, cycloalkylamines showed higher potency as the ring size grew from 4 (**25**, IC<sub>50</sub> = 83 nM) to 6 (**27**, IC<sub>50</sub> = 17 nM) and 7 (**28**, IC<sub>50</sub> = 19 nM). Comparable potency to cyclohexylamine **27** was observed with tetrahydropyranamine **29**. However, cyclic tertiary amines at C-1 position showed 5- to 10-fold loss of activity compared to the cycloalkylamines of the same ring size (**30**, **31**). It was also found that acyclic tertiary amines such as **32** were not tolerated at this position, indicating that these bulky amines either had steric clash with the enzyme or adopted an unfavorable conformation.

Table 2. Initial SAR of Amino Derivatives at C-1 of the Core



|    | R   | JAK2 IC <sub>50</sub> (nM) |
|----|---|----------------------------|
| 18 |    | 210                        |
| 3  |    | 230                        |
| 19 |    | 68                         |
| 20 |    | 49                         |
| 21 |    | 100                        |
| 22 |    | 74                         |
| 23 |    | 52                         |
| 24 |   | 210                        |
| 25 |  | 83                         |
| 26 |  | 51                         |
| 27 |  | 17                         |
| 28 |  | 19                         |
| 29 |  | 18                         |
| 30 |  | 230                        |
| 31 |  | 190                        |
| 32 |  | 2,700                      |

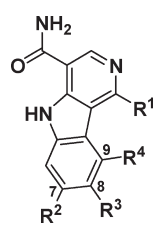
**Exploration of the C-Ring Substituents.** Having identified promising alkylamines at the 1-position of the A-ring that gave modest JAK2 activities, we next focused on substituents on the C-ring to further improve the potency. Initially, with cyclohexylamine at the 1-position of the A-ring, various substituents such as halogen, alkyl, aryl, and heteroaryl groups were explored on different positions of the C-ring (Table 3). As expected, substituents at the 6-position of the C-ring were not tolerated, indicating that they were too close to the hinge region of the enzyme and caused steric clash (data not shown). Compared to the unsubstituted

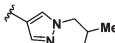
C-ring (33), the 7-chloro analogue 34 showed 2-fold improved JAK2 potency. On the other hand, the 9-chloro analogue 35 was 2-fold less potent than 33, presumably because of unfavorable steric clash of the 9-chloro group with the C-1 amine, which could cause conformational changes of the amine group. These findings led us to explore primarily the 7- and 8-positions of the C-ring, which are pointing toward the solvent exposed region of the protein based on modeling. Exploration of various aryl and heteroaryl groups on the 7- and 8-position revealed a strong and consistent preference for the 7-position over the 8-position (compare 36, 38 vs 37, 39). A remarkable potency improvement was achieved with heteroaryl groups such as 38 (IC<sub>50</sub> = 5 nM) at the 7-position. Further screening of pyrazoles, the 1*H*-pyrazol-4-yl analogue 40 and the 1*H*-pyrazol-5-yl analogue 41, revealed that these pyrazole analogues were less potent than the 1-methyl-1*H*-pyrazol-4-yl analogue 38 by 2- and 4-fold, respectively.

Although cyclohexylamine 27 presented the highest JAK2 activity out of the various amine groups initially tested (Table 2), key C-ring analogues of other promising amines at the 1-position were investigated in parallel in the context of potency, kinase selectivity, off-target activities, and PK properties. As a general trend, the (2*S*)-3,3-dimethylbutan-2-amine analogues at the 1-position such as 42 (IC<sub>50</sub> = 5 nM) showed JAK2 activities comparable to those of the corresponding cyclohexylamine analogues (Table 3). Moreover, the (2*S*)-3,3-dimethylbutan-2-amine analogues (e.g., 42, hERG<sup>20</sup> IC<sub>50</sub> = 29 000 nM, 49% inhibition of CYP3A4 at 10 μM) offered better off-target activities than the cyclohexylamine analogues (e.g., 38, hERG IC<sub>50</sub> = 620 nM, 75% inhibition of CYP3A4 at 10 μM). As a result, further screening of heterocycles on the C-ring was performed with the (2*S*)-3,3-dimethylbutan-2-amine group at the 1-position of the A-ring (Table 3). The isobutylpyrazole group (43) was not well tolerated and resulted in 8-fold loss of activity compared to 42. However, other heterocycles such as 44, 45, 46, and 47 generally maintained high JAK2 activity. These results were consistent with the X-ray cocrystal structure of 38 (Figure 3), which showed a preference for polar substituents at the 7-position that were pointing toward the solvent exposed region. The solvent exposed region was flexible enough to accommodate various polar groups while maintaining high potency. These findings also indicated that SAR studies in this region could be employed at later stage of the lead optimization in fine-tuning PK properties, off-target activities, or physical properties without affecting the already optimized JAK2 activity.

**Effect of the C-1 Amines on PK Properties.** While we were optimizing JAK2 potency, kinase selectivity, and off-target activities of the series, we were also closely monitoring the PK properties of the molecules. Although key (2*S*)-3,3-dimethylbutan-2-amines such as 42 revealed satisfactory properties in JAK2 potency and off-target activities, they displayed poor PK properties when they were dosed in rats (Cl<sub>p</sub> > Q<sub>h<sub>ep</sub></sub>). To understand the causes of their high plasma clearance, metabolic stability studies of the key compounds were performed (Figure 2). When compound 42 was incubated in rat hepatocytes, both the hydroxyl analogue (42-1) and the aldehyde analogue (42-2) at the γ-position of the amine at the 1-position were identified as major metabolites. The corresponding carboxylic acid analogue (42-3) was observed as well, albeit in minor quantity. However, no metabolic degradation of the methylpyrazole such as demethylation at the 7-position was observed in this study. These results indicated that the (2*S*)-3,3-dimethylbutan-2-amine at the

Table 3. SAR on the C-Ring



|    | R <sup>1</sup>  | R <sup>2</sup>  | R <sup>3</sup>  | R <sup>4</sup> | JAK2 IC <sub>50</sub><br>(nM) |
|----|---|---|---|----------------|-------------------------------|
| 33 |    | H   | H   | H              | 59                            |
| 34 |    | Cl  | H   | H              | 23                            |
| 35 |    | H   | H   | Cl             | 110                           |
| 36 |    | Phenyl  | H   | H              | 70                            |
| 37 |    | H   | Phenyl  | H              | 180                           |
| 38 |    |    | H   | H              | 5                             |
| 39 |  | H   |  | H              | 13                            |
| 40 |  |  | H   | H              | 13                            |
| 41 |  |  | H   | H              | 23                            |
| 42 |  |  | H   | H              | 5                             |
| 43 |  |  | H   | H              | 41                            |
| 44 |  |  | H   | H              | 12                            |
| 45 |  |  | H   | H              | 12                            |
| 46 |  |  | H   | H              | 14                            |
| 47 |  |  | H   | H              | 10                            |

1-position was the soft spot in hepatic first pass metabolism and might account for the high clearance of **42** in rats.

Identification of the metabolic instability of the *tert*-butyl group of the (2*S*)-3,3-dimethylbutan-2-amine prompted us to replace the *tert*-butyl group with other groups that are less prone to metabolic oxidation. It is known that cyclopropyl groups are more resistant to hydrogen abstraction than alkyl groups, thereby

more stable in metabolic oxidation.<sup>30,31</sup> With the methylpyrazole group at the 7-position, a handful of cyclopropyl containing amines were explored at the 1-position (Table 4). Gratifyingly, the (1*S*)-1-cyclopropylethanamine analogue **48** showed marked improvement in PK properties in rats ( $Cl_p = 44$  mL/min/kg,  $t_{1/2} = 1.0$  h) compared to **42**. Rat hepatocyte incubation study also revealed improved metabolic stability of **48** over **42**

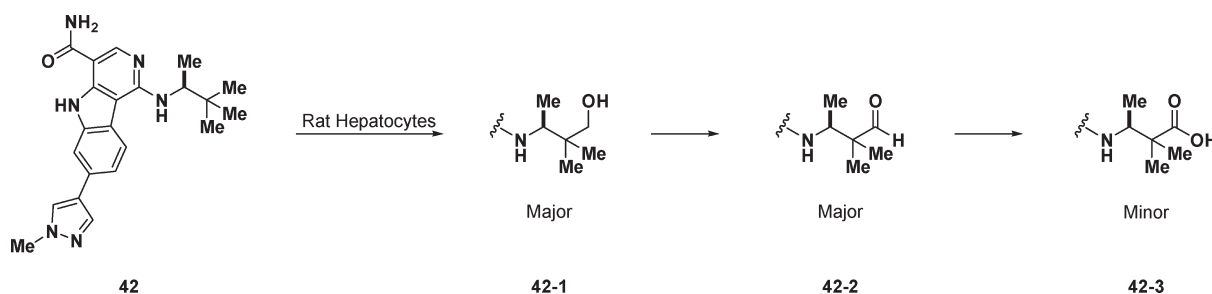


Figure 2. Major metabolites of 42 in rat hepatocytes.

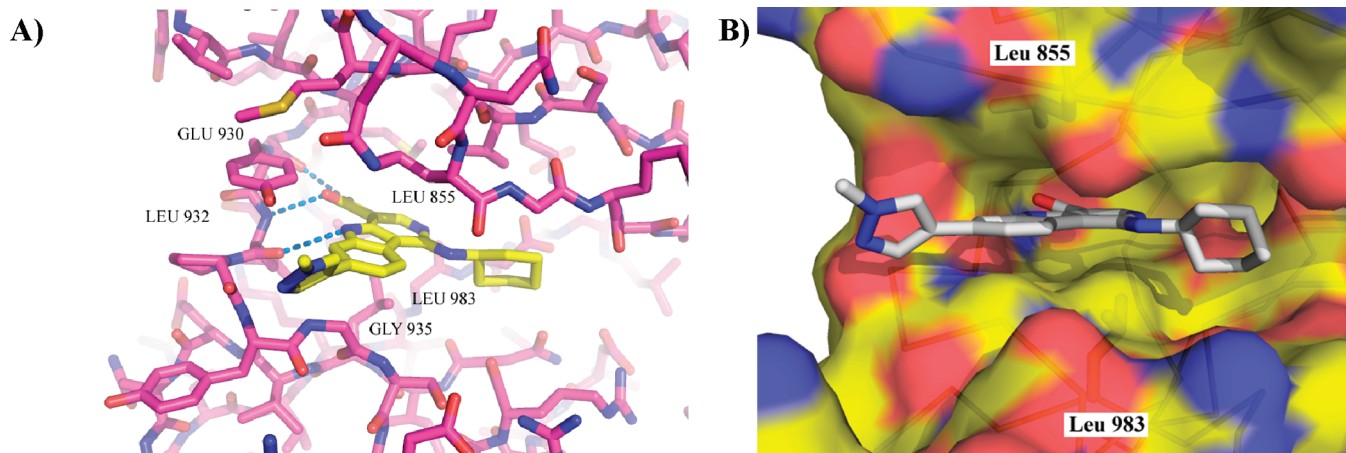


Figure 3. X-ray crystal structure of 38 bound to JAK2: (A) hydrogen-bonding pattern in the structure of 38 bound to JAK2; (B) surface view of the JAK2 active site bound to 38.

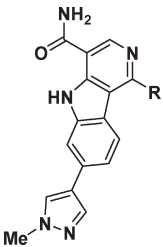
( $t_{1/2} = 61$  and 15 min, respectively). Although the cyclopropyl group was introduced in place of the *tert*-butyl group in order to primarily improve PK properties, the replacement provided surprisingly high enhancement in JAK2 potency as well ( $IC_{50} = 1$  nM). More importantly, 48 showed 25-fold higher potency than 42 ( $IC_{50} = 14$  nM vs 370 nM) in the cell-biochemical assay, inhibition of phosphorylation of STAT5 (pSTAT5), downstream of JAK. As seen with the 3,3-dimethylbutan-2-amine analogues (23, 24 in Table 2), the (*R*)-enantiomer 49 displayed a 10-fold loss in JAK2 potency compared to 48. These encouraging results led us to further explore the  $\alpha$ -branched alkyl group of the amine both sterically and electronically. While the ethyl analogue 50 displayed comparable potency in both JAK2 and pSTAT5, 50 showed high plasma clearance in rats ( $Cl_p > Q_{hep}$ ), indicating that the ethyl group might be rapidly metabolized. Bulkier alkyl groups such as isopropyl group at the  $\alpha$ -branch (51) showed a tendency to lose potency as the alkyl group grew bulkier. As a relatively small and metabolically stable substituent, 1,1-dicyclopropylmethanamine was introduced to the A-ring and tested in rats. Although pSTAT5 potency of 52 was suboptimal, it offered further improved plasma clearance and half-life ( $Cl_p = 22$  mL/min/kg,  $t_{1/2} = 3.2$  h).

Next,  $\alpha$ -branched alkyl groups with electron withdrawing atoms were pursued. Having identified that oxidative metabolism of the amino group at the 1-position was the major cause of high clearance, it was anticipated that electron withdrawing atoms on the amino group might make the molecule less susceptible to oxidative metabolism, thereby improving PK properties. To this end, a trifluoromethyl group was introduced in place of the

$\alpha$ -methyl group of the amine retaining the cyclopropyl group (Table 4). Indeed, the (*R*)-1-cyclopropyl-2,2,2-trifluoroethanamine analogue 53 displayed significantly improved PK properties in rats ( $Cl_p = 14$  mL/min/kg,  $t_{1/2} = 4.1$  h, bioavailability of 65%), albeit it showed a higher cell shift compared to 48. As seen previously, a stark difference in potency between the two enantiomers (53, 54) was observed as well. When the cyclopropyl group was replaced with isopropyl or cyclobutyl groups as in 55 and 56, the compounds suffered from high rat clearance, indicating that the electron withdrawing trifluoromethyl group was not sufficient in preventing rapid metabolism of the molecules. Interestingly, 1-amino-7-(1-methyl-1*H*-pyrazol-4-yl)-5*H*-pyrido[4,3-*b*]indole-4-carboxamides in general displayed high JAK2 selectivity over JAK3 (typically >50-fold).

**Optimization of the C-7 Heterocycles.** Although compounds 52 and 53 displayed optimal JAK2 biochemical potency and rat PK properties, their off-target activities such as hERG activity<sup>20</sup> and CYP enzyme inhibition were found to be suboptimal (hERG  $IC_{50}$  of 1700 and 3400 nM; 80% and 66% inhibition of CYP2C9 at 10  $\mu$ M for 52 and 53, respectively). As previously discussed, we envisioned that we could further improve off-target activities, physical properties, and PK properties while maintaining high JAK2 potency by fine-tuning substituents at the 7-position. An array of heterocycles were explored at the 7-position with either 1,1-dicyclopropylmethanamine or (*R*)-1-cyclopropyl-2,2,2-trifluoroethanamine at the 1-position as summarized in Table 5. The 1*H*-pyrazol-4-yl analogues 57 and 61 displayed superior cell potency and comparable rat clearance to 52 and 53. However, 57 and 61 had the same level of hERG

Table 4. SAR of Amines at the 1-Position with Methylpyrazole at the 7-Position



|    | R   | JAK2 IC <sub>50</sub><br>(nM) | JAK3 IC <sub>50</sub><br>(nM) | pSTAT5 IC <sub>50</sub><br>(nM) | Rat Cl <sub>p</sub> <sup>a</sup><br>(mL/min/kg) |
|----|---|-------------------------------|-------------------------------|---------------------------------|---|
| 42 |    | 5                             | 350                           | 370                             | > Q <sub>hep</sub> <sup>b,c</sup>               |
| 48 |    | 1                             | 140                           | 14                              | 44 <sup>e</sup>                                 |
| 49 |    | 11                            | 740                           | 79                              | ND <sup>d</sup>                                 |
| 50 |    | 2                             | 170                           | 45                              | > Q <sub>hep</sub> <sup>b,c</sup>               |
| 51 |    | 3                             | 210                           | 95                              | ND <sup>d</sup>                                 |
| 52 |  | 2                             | 280                           | 130                             | 22 <sup>b</sup>                                 |
| 53 |  | 0.4                           | 230                           | 41                              | 14 <sup>e</sup>                                 |
| 54 |  | 9                             | 1,900                         | 530                             | ND <sup>d</sup>                                 |
| 55 |  | 3                             | 560                           | ND                              | > Q <sub>hep</sub> <sup>c,f</sup>               |
| 56 |  | 12                            | 1,700                         | 350                             | > Q <sub>hep</sub> <sup>c,e</sup>               |

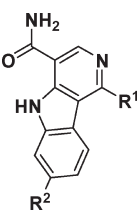
<sup>a</sup> iv at 1 mg/kg. <sup>b</sup> Dosed as a solution in PEG400/40% Captisol (50:50 (v/v)). <sup>c</sup> Q<sub>hep</sub> = hepatic blood flow. <sup>d</sup> ND = not determined. <sup>e</sup> Dosed as a solution in PEG400/40% Trappsol (50:50 (v/v)). <sup>f</sup> Dosed as a solution in PEG400/50% Captisol (50:50 (v/v)).

and CYP activities as **52** and **53** (Table 6). The pyridazine analogues **58** and **64** displayed high rat clearances, while compound **63** showed more than 10-fold loss of potency. Although the 2-pyrazine analogue **59** showed cell potency comparable to that of **52**, it displayed greater than 2-fold higher potency in hERG activity. Major improvement in rat clearance was seen with the 2-aminopyridine analogue **62** (Cl<sub>p</sub> = 6 mL/min/kg), albeit it suffered from submicromolar hERG activity. The 2-aminopyrimidine analogue of **52** (**60**) displayed a balanced profile in JAK2 potency (pSTAT IC<sub>50</sub> = 29 nM), rat PK properties (Cl<sub>p</sub> = 21 mL/min/kg), and off-target activities. Eventually, excellent rat clearance and clean off-target activities were achieved with the 2-aminopyrimidine analogue **65** (Cl<sub>p</sub> = 7 mL/min/kg, hERG IC<sub>50</sub> = 22 000 nM, CYP3A4 and CYP2C9 of <50% inhibition at 10 μM). Compound **65** offered superior cell potency (pSTAT IC<sub>50</sub> = 25 nM) while maintaining high selectivity over JAK3 (>300-fold) compared to **53**. Moreover, **65** displayed high

enzymatic and cell potency against JAK2<sup>V617F</sup> (JAK2<sup>V617F</sup> IC<sub>50</sub> = 0.4 nM, pSTAT5 (BaF3)<sup>V617F</sup> IC<sub>50</sub> = 11 nM), which would suggest its efficacy in the treatment of JAK2<sup>V617F</sup> driven MPDs.<sup>34</sup>

**Crystal Structure of Compound 38.** An X-ray crystal structure of a representative of this series, **38**, bound to JAK2 revealed the expected mode of binding (Figure 3). Compound **38** interacts with the DFG-in form of JAK2 by binding in the ATP site. The 5H-pyrido[4,3-*b*]indol core is clamped by hydrophobic interactions with the side chain of Leu855 from the N-lobe and Leu983 and the α-carbon of Gly935 from the C-lobe (Figure 3B). Compound **38** is oriented so that the methylpyrazole points toward solvent and the cyclohexane points back toward the DFG motif, sitting in a pocket 4 Å from Asp994 of the DFG motif. Compound **38** makes three hydrogen bonds to backbone atoms of the kinase hinge (Figure 3A). The carboxamide oxygen makes a hydrogen bond with the backbone amine of Leu932 (2.9 Å), and the carboxamide nitrogen forms a hydrogen

Table 5. SAR of Heterocycles at the 7-Position



|    | R <sup>1</sup> | R <sup>2</sup> | JAK2 IC <sub>50</sub><br>(nM) | JAK3 IC <sub>50</sub><br>(nM) | pSTAT5 IC <sub>50</sub><br>(nM) | Rat Cl <sub>p</sub> <sup>a</sup><br>(mL/min/kg) |
|----|----------------|----------------|-------------------------------|-------------------------------|---------------------------------|---|
| 57 |                |                | 3                             | 220                           | 40                              | 31 <sup>b</sup>                                 |
| 58 |                |                | 2                             | 270                           | 28                              | > Q <sub>hep</sub> <sup>c,e</sup>               |
| 59 |                |                | 4                             | 640                           | 100                             | ND <sup>d</sup>                                 |
| 60 |                |                | 1                             | 220                           | 29                              | 21 <sup>f</sup>                                 |
| 61 |                |                | 1                             | 220                           | 32                              | 21 <sup>e</sup>                                 |
| 62 |                |                | 2                             | 370                           | 61                              | 6 <sup>e</sup>                                  |
| 63 |                |                | 8                             | 430                           | 530                             | 15 <sup>b</sup>                                 |
| 64 |                |                | 2                             | 160                           | 120                             | 54 <sup>b</sup>                                 |
| 65 |                |                | 0.8                           | 300                           | 25                              | 7 <sup>f</sup>                                  |

<sup>a</sup> iv at 1 mg/kg. <sup>b</sup> Dosed as a solution in PEG400/40% Captisol (50:50 (v/v)). <sup>c</sup> Q<sub>hep</sub> = hepatic blood flow. <sup>d</sup> ND = not determined. <sup>e</sup> Dosed as a solution in PEG400/40% Trappsol (50:50 (v/v)). <sup>f</sup> Dosed as a solution in PEG400/Trappsol/water (35:60:5 (v/v/v)).

Table 6. Off-Target Activities of Selected JAK2 Inhibitors

| compd | hERG<br>IC <sub>50</sub> (nM) | CYP3A4 inhibition at<br>10 μM (%) | CYP2C9 inhibition at<br>10 μM (%) |
|-------|-------------------------------|-----------------------------------|-----------------------------------|
| 52    | 1,700                         | 62                                | 80                                |
| 53    | 3,400                         | 48                                | 66                                |
| 57    | 990                           | 66                                | 80                                |
| 59    | 720                           | 65                                | 46                                |
| 60    | 8,200                         | 55                                | 35                                |
| 61    | 3,000                         | 68                                | 61                                |
| 62    | 750                           | 65                                | 41                                |
| 65    | 22,000                        | 30                                | 34                                |

bond with the carbonyl oxygen of Glu930 (3.0 Å). The third hydrogen bond with the hinge is between the indole nitrogen of 38 and the carbonyl oxygen of Leu932 (3.2 Å).

**PK and off-Target Activity Profile of 65.** Encouraged by the superior cell potency, low rat clearance, and clean hERG<sup>20</sup> and CYP activities of 65, we next fully characterized 65 in PK

properties and off-target activities in order to assess its potential as a preclinical candidate. As shown in Table 7, 65 displayed a balanced PK profile across species: low to moderate Cl<sub>p</sub>, long half-life (≥ 4.5 h), and high bioavailability (≥ 66%) suitable for oral dosing. In addition to favorable PK properties, 65 offered clean ion channel activities (IC<sub>50</sub> values for I<sub>Kr</sub>, I<sub>Ks</sub>,<sup>20</sup> Ca<sub>v</sub>1.2,<sup>32</sup> Na<sub>v</sub>1.5<sup>33</sup> of >10, >10, >30, >30 μM, respectively). It was also completely clean in CYP enzyme inhibitory activities (IC<sub>50</sub> > 75 μM for each CYP3A4, 2C9, 2D6), indicating that it has very low potential for drug–drug interactions. Throughout the SAR, selectivity profile against a broad panel of kinases was closely monitored for key inhibitors in order to assess potential in vivo adverse events caused by inhibiting off-target kinases. In general, lead inhibitors in this series showed high selectivity against JAK3 (vide supra), whereas they displayed similar inhibitory activities of JAK1 and JAK2 (e.g., JAK1 IC<sub>50</sub> = 1.5 nM for 65). When 65 was tested against a panel of 220 kinases, it displayed greater than 25-fold selectivity against 198 kinases. Twenty-two nonmutant kinases whose IC<sub>50</sub> values were within 25-fold of JAK2 IC<sub>50</sub> are shown in Table 8.

**Table 7. PK Profile of Compound 65 in Preclinical Species<sup>a</sup>**

| iv parameters   | rat | dog | monkey |
|---|-----|-----|--------|
| dose (mpk)  | 1   | 0.5 | 0.5    |
| AUC <sub>norm</sub> ( $\mu\text{M}\cdot\text{h}/\text{mpk}$ ) | 5.3 | 2.4 | 5.2    |
| Cl <sub>p</sub> (mL/min/kg)                                   | 7.4 | 18  | 7.4    |
| V <sub>dss</sub> (L/kg)                                       | 2.5 | 6.1 | 4.7    |
| t <sub>1/2</sub> (h)  | 4.5 | 5.2 | 7.3    |
| po parameters   | rat | dog | monkey |
| dose (mg/kg)  | 2   | 1   | 1      |
| AUC <sub>norm</sub> ( $\mu\text{M}\cdot\text{h}/\text{mpk}$ ) | 3.4 | 2.5 | 3.4    |
| C <sub>max</sub> ( $\mu\text{M}$ )                            | 0.6 | 0.3 | 0.2    |
| t <sub>max</sub> (h)  | 6.0 | 5.1 | 6.0    |
| F <sup>b</sup> (%)  | 67  | 120 | 66     |

<sup>a</sup> n = 3. Dosed as a solution in PEG400/Trappsol/water (35:60:5 (v/v/v)). mpk = mg/kg. <sup>b</sup> Bioavailability.

**Table 8. Kinase Selectivity Profile of 65**

| kinase <sup>a</sup> | fold selectivity <sup>b</sup> | kinase <sup>a</sup> | fold selectivity <sup>b</sup> |
|---------------------|-------------------------------|---------------------|-------------------------------|
| cSRC                | 1                             | ARK5                | 6                             |
| TrkA                | 1                             | BTK                 | 7                             |
| ACK1                | 2                             | Yes                 | 7                             |
| Fms                 | 2                             | PTK5                | 8                             |
| Fyn                 | 2                             | TrkB                | 8                             |
| Flt3                | 3                             | CaMKII $\delta$     | 10                            |
| Hck                 | 3                             | CaMKII $\gamma$     | 11                            |
| Ret                 | 3                             | PRK2                | 13                            |
| Bmx                 | 4                             | Arg                 | 17                            |
| Lyn                 | 4                             | MLK1                | 18                            |
| Fgr                 | 5                             | ALK                 | 25                            |
| Lck                 | 5                             |                     |                               |

<sup>a</sup> Human enzyme. <sup>b</sup> Fold selectivity against in-house JAK2 IC<sub>50</sub> of 65 (0.8 nM).

**In Vivo Studies of 65.** On the basis of excellent on-target potency, off-target selectivity profile, and PK profile in three species, compound 65 was chosen for further in vivo evaluation. Compound 65 was studied in mouse models to assess its in vivo target engagement and efficacy.<sup>34</sup> When 65 was orally administered to C57Bl/6 mice stimulated with darbepoetin, pSTAT5 was reduced in a dose-dependent manner (in vivo IC<sub>50</sub> = 1.2  $\mu\text{M}$ ). In the darbepoetin-induced PV model, 65 successfully prevented the elevation of both hematocrit and spleen weight in a dose-dependent manner, demonstrating its efficacy at preventing acute development of PV driven by wild-type JAK2. The effect of 65 on major lymphoid populations was investigated as well to assess its potential adverse effects. The details of these studies and results will be published in a future article.

## CONCLUSIONS

The development of a series of 1-amino-5H-pyrido[4,3-b]indol-4-carboxamides as ATP-competitive JAK2 inhibitors was achieved by systematic optimization of multiple substituents around the core structure. A series of SAR studies identified the 1- and 7-positions of the core as the optimal positions for substitution, which led to the identification of inhibitors with subnanomolar

JAK2 activities. Incorporation of (R)-1-cyclopropyl-2,2,2-trifluoroethanamine at the 1-position was found to be crucial to achieving excellent cell activity and PK profile. In addition, the 2-aminopyrimidine group at the 7-position eliminated off-target liabilities such as hERG activity and P450 inhibitory activities in this series. These efforts culminated with the discovery of 7-(2-aminopyrimidin-5-yl)-1-[[[(1R)-1-cyclopropyl-2,2,2-trifluoroethyl]amino]-5H-pyrido[4,3-b]indole-4-carboxamide (65), a potent, selective, and orally active inhibitor of JAK2 and JAK2<sup>V617F</sup> with an excellent PK profile in three preclinical species. Furthermore, compound 65 displayed in vivo target engagement and good efficacy at preventing PV-like disease in mouse models.

## EXPERIMENTAL SECTION

**Chemistry.** Commercial reagents were obtained from reputable suppliers and used as received. All solvents were purchased in septum-sealed bottles stored under an inert atmosphere. All reactions were sealed with septa through which an argon atmosphere was introduced unless otherwise noted. Liquid reagents and solvents were transferred under a positive pressure of nitrogen via syringe. Reactions were conducted in microwave vials or round bottomed flasks containing Teflon-coated magnetic stir bars. Microwave reactions were performed with a Biotage Initiator series microwave (fixed hold time setting; reaction temperatures monitored by the internal infrared sensor).

Reactions were monitored by thin layer chromatography (TLC) on precoated TLC glass plates (silica gel 60 F254, 250  $\mu\text{m}$  thickness) or by LC/MS (30 mm  $\times$  2 mm, 2  $\mu\text{m}$  column + guard; 2  $\mu\text{L}$  injection; 3–98% MeCN/water + 0.05% TFA gradient over 2.3 min; 0.9 mL/min flow; ESI; positive ion mode; UV detection at 254 nm). Visualization of the developed TLC chromatogram was performed by fluorescence quenching. Flash chromatography was performed on an automated purification system using prepacked silica gel columns. <sup>1</sup>H NMR spectra were recorded on either a 500 or a 600 MHz Varian spectrometer. Chemical shifts ( $\delta$ ) are reported relative to residual proton solvent signals. Data for NMR spectra are reported as follows: chemical shift ( $\delta$  ppm), multiplicity (s = singlet, brs = broad singlet, d = doublet, t = triplet, q = quartet, dd = doublet of doublets, td = triplet of doublets, m = multiplet), coupling constant (Hz), integration.

All tested compounds reported are of at least 95% purity, as judged by LCAP (150 mm  $\times$  4.6 mm i.d., 5  $\mu\text{m}$  column; 5  $\mu\text{L}$  injection; 10–100% MeCN/H<sub>2</sub>O + 0.05% TFA gradient over 6.75 min; 1 mL/min flow; ESI; positive ion mode; UV detection at 254 nm, Bw8).

**8-Fluoro-2,5-dihydro-1H-pyrido[4,3-b]indol-1-one (8a).** To a separatory funnel was added 4-fluorophenylhydrazine hydrochloride (9a, 92 g, 565 mmol) and sodium hydroxide (1.0 M in H<sub>2</sub>O, 600 mL, 600 mmol). The suspension was shaken and then diluted with ethyl acetate and brine. The organic layer was separated, dried over magnesium sulfate, filtered, and concentrated. To the resulting liquid were added 2,4-dihoxypyridine (20.00 g, 180 mmol) and diphenyl ether (200 mL). A Dean–Stark trap was fitted atop the flask, and the mixture was heated to 175 °C for 90 min. The mixture was then heated to 300 °C for 1 h. When the mixture was cooled, toluene (500 mL) was added and the solid that precipitated was collected by filtration. The filter cake was washed with toluene (500 mL) and then broken up with a mortar and pestle. The solid was then suspended in hot dioxane (100 °C), filtered and the filter cake was washed with toluene to afford 8a (24.1 g, 119 mmol, 66% yield). LRMS (ESI) calcd for (C<sub>11</sub>H<sub>8</sub>FN<sub>2</sub>O) [M + H]<sup>+</sup> 203.1, found 203.1. <sup>1</sup>H NMR (600 MHz, DMSO-d<sub>6</sub>)  $\delta$  11.77 (s, 1H), 11.12 (s, 1H), 7.70 (dd, J = 2.4, 9.3 Hz, 1H), 7.45 (dd, J = 4.3, 8.7 Hz, 1H), 7.29 (t, J = 6.2 Hz, 1H), 7.10 (td, J = 2.1, 8.8 Hz, 1H), 6.47 (d, J = 7.0 Hz, 1H).

**7-Chloro-2,5-dihydro-1H-pyrido[4,3-*b*]indol-1-one (8c).** A mixture of 3-chlorophenylhydrazine hydrochloride (**9b**, 165 g, 922 mmol) and 6 N NaOH (150 mL, 900 mmol) in ethanol (800 mL) was extracted with ethyl acetate (2 L). The organic layer was concentrated, and the residue was diluted with dichloromethane. The organic layer was separated, dried over magnesium sulfate, and concentrated. To 2, 4-dihydropyridine (50.9 g, 458 mmol) in phenyl ether (800 mL) in a three-neck flask fitted with a Dean–Stark trap was added 3-chlorophenylhydrazine. The reaction mixture was heated to 175 °C for 1 h and then to 230 °C for 3 h. The reaction mixture was allowed to cool to room temperature. The resultant slurry was filtered and washed with toluene. The collected solids were ground to a fine powder, slurried in MeOH (200 mL), and sonicated for 15 min. The slurry was filtered, washed with MeOH, and dried to afford **8c** (40.9 g, 187 mmol, 41% yield). <sup>1</sup>H NMR of the filtrate indicated that **8b** was the major component in the filtrate. LRMS (ESI) calcd for (C<sub>11</sub>H<sub>8</sub>ClN<sub>2</sub>O) [M + H]<sup>+</sup> 219.0, found 219.0. <sup>1</sup>H NMR (600 MHz, DMSO-*d*<sub>6</sub>) δ 11.82 (s, 1H), 11.18 (s, 1H), 8.04 (d, *J* = 8.3 Hz, 1H), 7.51 (d, *J* = 1.7 Hz, 1H), 7.31 (d, *J* = 7.0 Hz, 1H), 7.18 (dd, *J* = 1.8, 8.4 Hz, 1H), 6.50 (d, *J* = 7.0 Hz, 1H).

**4-Bromo-8-fluoro-2,5-dihydro-1H-pyrido[4,3-*b*]indol-1-one (7a).** To a solution of **8a** (1.00 g, 4.95 mmol) in DMF (15.0 mL) was added *N*-bromosuccinimide, and the mixture was allowed to stir in the dark for 1 h at room temperature. The solution was then concentrated and column chromatography on silica gel was used for purification to afford **7a** (0.91 g, 3.24 mmol, 66% yield). LRMS (ESI) calcd for (C<sub>11</sub>H<sub>7</sub>BrFN<sub>2</sub>O) [M + H]<sup>+</sup> 281.0, found 280.9. <sup>1</sup>H NMR (600 MHz, DMSO-*d*<sub>6</sub>) δ 12.05 (s, 1H), 11.48 (s, 1H), 7.72 (dd, *J* = 2.7, 9.2 Hz, 1H), 7.59 (s, 1H), 7.53 (dd, *J* = 4.5, 8.9 Hz, 1H), 7.21–7.15 (m, 1H).

**4-Bromo-7-chloro-2,5-dihydro-1H-pyrido[4,3-*b*]indol-1-one (7b).** To a stirred solution of **8c** (15.1 g, 69.1 mmol) in DMF (112 mL) was added NBS (12.3 g, 69.1 mmol) in small portions at 0 °C. The reaction mixture was covered with aluminum foil and warmed to room temperature. The mixture was left to stir for 2 h, treated with water (112 mL), and left to stir for 2 h. The reaction mixture was filtered and washed with water. The solid was placed in a flask, and water (250 mL) was added. The resultant slurry was stirred at 50 °C overnight, filtered, and dried to afford **7b** (16.2 g, 54.3 mmol, 79% yield). LRMS (ESI) calcd for (C<sub>11</sub>H<sub>7</sub>BrClN<sub>2</sub>O) [M + H]<sup>+</sup>, 296.9, found 296.9. <sup>1</sup>H NMR (600 MHz, DMSO-*d*<sub>6</sub>) δ 12.09 (s, 1H), 11.04 (s, 1H), 8.05 (d, *J* = 8.5 Hz, 1H), 7.92 (s, 1H), 7.60 (d, *J* = 8.8 Hz, 1H), 7.53 (d, *J* = 1.9 Hz, 1H).

**4-Bromo-1-chloro-8-fluoro-5H-pyrido[4,3-*b*]indole (10a).** A suspension of **7a** (1.10 g, 3.91 mmol) in phosphorus oxychloride (16.45 g, 10 mL, 107 mmol) was irradiated in the microwave at 175 °C for 15 min. The solution was then poured over ice and diluted with water. The solution was neutralized by the slow addition of NaOH (6 M and then 11 M in water). The mixture was extracted with ethyl acetate (3×) and the combined organic layers were dried over magnesium sulfate, filtered, and concentrated to afford **10a** (1.00 g, 3.34 mmol, 85% yield). LRMS (ESI) calcd for (C<sub>11</sub>H<sub>6</sub>BrClFN<sub>2</sub>) [M + H]<sup>+</sup> 300.9, found 300.9. <sup>1</sup>H NMR (600 MHz, DMSO-*d*<sub>6</sub>) δ 12.55 (s, 1H), 8.41 (s, 1H), 8.04 (dd, *J* = 2.6, 9.2 Hz, 1H), 7.68 (dd, *J* = 4.5, 8.9 Hz, 1H), 7.48 (td, *J* = 2.6, 9.1 Hz, 1H).

**4-Bromo-1,7-dichloro-5H-pyrido[4,3-*b*]indole (10b).** A suspension of **7b** (4.89 g, 16.4 mmol) in phosphorus oxychloride (10.5 mL, 113 mmol) was irradiated in the microwave at 175 °C for 15 min. The reaction mixture was then cooled to room temperature, poured over ice, and treated with 11 M sodium hydroxide (100 mL). The mixture was extracted with ethyl acetate (3×). The combined organic layers were dried with magnesium sulfate, filtered, and concentrated under reduced pressure to give **10b** (4.21 g, 13.3 mmol, 81%). LRMS (ESI) calcd for (C<sub>11</sub>H<sub>6</sub>BrCl<sub>2</sub>N<sub>2</sub>) [M + H]<sup>+</sup> 316.9, found 316.9. <sup>1</sup>H NMR (600 MHz, DMSO-*d*<sub>6</sub>) δ 12.61 (s, 1H), 8.43 (s, 1H), 8.33 (d, *J* = 8.5 Hz, 1H), 7.66 (d, *J* = 1.9 Hz, 1H), 7.43 (dd, *J* = 1.9, 8.5 Hz, 1H).

**8-Fluoro-1-oxo-2,5-dihydro-1H-pyrido[4,3-*b*]indole-4-carbonitrile (13a).** To a solution of **7a** (75 mg, 0.27 mmol) in NMP (2 mL) was added copper(I) cyanide (34 mg, 0.37 mmol), and the mixture was irradiated in the microwave at 225 °C for 40 min. Then the solution was poured into a 10:1 (v/v) mixture of ethyl acetate/hexanes and filtered through a silica gel plug. The filtrate was concentrated, taken up in ethyl acetate, washed with brine, dried over magnesium sulfate, filtered, and concentrated. Purification by chromatography on silica gel afforded **13a** (30 mg, 0.13 mmol, 50% yield). LRMS (ESI) calcd for (C<sub>12</sub>H<sub>7</sub>FN<sub>3</sub>O) [M + H]<sup>+</sup> 228.0, found 228.0. <sup>1</sup>H NMR (600 MHz, CD<sub>3</sub>OD) δ 8.06 (s, 1H), 7.90–7.81 (m, 2H), 7.56–7.52 (m, 2H), 7.17 (ddd, *J* = 2.6, 9.3, 18.4 Hz, 1H).

**7-Chloro-1-oxo-2,5-dihydro-1H-pyrido[4,3-*b*]indole-4-carbonitrile (13b).** To a mixture of **7b** (1.42 g, 4.77 mmol) and tetrakis-(triphenylphosphine)palladium (551 mg, 0.477 mmol) in DMF (23.9 mL) was added zinc cyanide (280 mg, 2.39 mmol). The flask was sealed and purged with nitrogen gas for 5 min. The reaction mixture was stirred at 100 °C for 16 h. The mixture was cooled, diluted with ethyl acetate, and washed with saturated sodium bicarbonate. The organic layer was dried with magnesium sulfate, filtered, and concentrated under reduced pressure. The residue was purified by chromatography on silica gel to afford **13b** (860 mg, 3.53 mmol, 74% yield) as a brown solid. LRMS (ESI) calcd for (C<sub>12</sub>H<sub>7</sub>ClN<sub>3</sub>O) [M + H]<sup>+</sup> 244.0, found 244.0. <sup>1</sup>H NMR (600 MHz, DMSO-*d*<sub>6</sub>) δ 12.63 (s, 1H), 12.16 (s, 1H), 8.27 (d, *J* = 6.6 Hz, 1H), 8.02 (d, *J* = 8.4 Hz, 1H), 7.56 (s, 1H), 7.27 (d, *J* = 8.4 Hz, 1H).

**1-Chloro-8-fluoro-5H-pyrido[4,3-*b*]indole-4-carbonitrile (6a).** A mixture of **13a** (50 mg, 0.22 mmol) in phosphorus oxychloride (3.29 g, 2 mL, 21.46 mmol) was irradiated in the microwave at 175 °C for 13 min. The solution was then cooled to ambient temperature and concentrated in vacuo. The residue was dissolved in ethyl acetate, washed with aqueous saturated sodium bicarbonate and brine, dried over magnesium sulfate, filtered, and concentrated. Purification by HPLC afforded **6a** (30 mg, 0.12 mmol, 56% yield). LRMS (ESI) calcd for (C<sub>12</sub>H<sub>6</sub>ClFN<sub>3</sub>) [M + H]<sup>+</sup> 246.0, found 246.0. <sup>1</sup>H NMR (600 MHz, DMSO-*d*<sub>6</sub>) δ 13.24 (s, 1H), 8.76 (s, 1H), 8.09 (dd, *J* = 2.5, 9.1 Hz, 1H), 7.69 (dd, *J* = 4.4, 8.9 Hz, 1H), 7.53 (td, *J* = 2.6, 9.1 Hz, 1H).

**1,7-Dichloro-5H-pyrido[4,3-*b*]indole-4-carbonitrile (6b).** To 7-chloro-1-oxo-2,5-dihydro-1H-pyrido[4,3-*b*]indole-4-carbonitrile (860 mg, 3.53 mmol) was added phosphorus oxychloride (2.25 mL, 24.2 mmol). The reaction mixture was heated to 175 °C for 15 min in a microwave. The mixture was cooled and poured over ice. The aqueous mixture was made basic by the addition of 6 and 11 M NaOH. The aqueous layer was extracted with ethyl acetate (3×). The combined organic layers were dried with magnesium sulfate, filtered, and concentrated under reduced pressure. The residue was purified by chromatography on silica gel to afford 1,7-dichloro-5H-pyrido[4,3-*b*]indole-4-carbonitrile (800 mg, 3.05 mmol, 86% yield) as an off white solid. LRMS (ESI) calcd for (C<sub>12</sub>H<sub>6</sub>Cl<sub>2</sub>N<sub>3</sub>) [M + H]<sup>+</sup> 262.0, found 262.0. <sup>1</sup>H NMR (600 MHz, DMSO-*d*<sub>6</sub>) δ 13.29 (s, 1H), 8.76 (s, 1H), 8.35 (d, *J* = 8.5 Hz, 1H), 7.67 (d, *J* = 1.7 Hz, 1H), 7.47 (dd, *J* = 1.9, 8.5 Hz, 1H).

**General Procedure for Amine Addition, Incorporation of Nitrile Followed by Hydrolysis. 1-(Butylamino)-8-fluoro-5H-pyrido[4,3-*b*]indole-4-carboxamide (20).** *Step 1.* A solution of **10a** (150 mg, 0.50 mmol) in butylamine (1.7 g, 24 mmol) was heated to 100 °C for 2 days. The reaction mixture was cooled to room temperature and purified by column chromatography on silica gel to afford 4-bromo-*N*-butyl-8-fluoro-5H-pyrido[4,3-*b*]indol-1-amine (115 mg, 0.342 mmol, 68% yield). LRMS (ESI) calcd for (C<sub>15</sub>H<sub>16</sub>BrFN<sub>3</sub>) [M + H]<sup>+</sup> 336.0, found 336.0. <sup>1</sup>H NMR (600 MHz, DMSO-*d*<sub>6</sub>) δ 11.79 (brs, 1H), 8.25 (dd, *J* = 2.3, 10.3 Hz, 1H), 8.00 (s, 1H), 7.54 (dd, *J* = 4.7, 8.8 Hz, 1H), 7.25 (td, *J* = 9.1, 2.4 Hz, 1H), 6.62 (brs, 1H), 3.54 (m, 2H), 1.64 (m, 2H), 1.38 (m, 2H), 0.92 (t, *J* = 7.5 Hz, 3H).

**Step 2.** To a solution of 4-bromo-*N*-butyl-8-fluoro-5*H*-pyrido[4,3-*b*]indol-1-amine (105 mg, 0.312 mmol) in NMP (1 mL) was added copper(I) cyanide (69.9 mg, 0.781 mmol), and the mixture was heated to 225 °C overnight. The reaction mixture was cooled to room temperature, diluted with ethyl acetate, washed with water, dried over magnesium sulfate, filtered, and concentrated. The residue was purified by flash chromatography to afford 1-(butylamino)-8-fluoro-5*H*-pyrido[4,3-*b*]indole-4-carbonitrile (68 mg, 0.24 mmol, 77% yield). LRMS (ESI) calcd for (C<sub>16</sub>H<sub>16</sub>FN<sub>4</sub>) [M + H]<sup>+</sup> 283.1, found 283.1. <sup>1</sup>H NMR (600 MHz, DMSO-*d*<sub>6</sub>) δ 12.40 (brs, 1H), 8.41 (s, 1H), 8.33 (dd, *J* = 10.3, 2.3 Hz, 1H), 7.53 (dd, *J* = 4.6, 9.0 Hz, 1H), 7.31 (brs, 1H), 7.27 (td, *J* = 9.1, 2.3 Hz, 1H), 3.64 (m, 2H), 1.65 (m, 2H), 1.38 (m, 2H), 0.93 (t, *J* = 7.5 Hz, 3H).

**Step 3.** To a mixture of 1-(butylamino)-8-fluoro-5*H*-pyrido[4,3-*b*]indole-4-carbonitrile (58 mg, 0.21 mmol) and potassium carbonate (77 mg, 0.56 mmol) in DMSO (3 mL) was added hydrogen peroxide (35%, 0.09 mL, 1.03 mmol), and the mixture was heated to 70 °C overnight. The reaction mixture was cooled to room temperature, filtered, and purified by HPLC to afford **20** (50 mg, 0.17 mmol, 81% yield). LRMS (ESI) calcd for (C<sub>16</sub>H<sub>18</sub>FN<sub>4</sub>O) [M + H]<sup>+</sup> 301.1, found 301.1. <sup>1</sup>H NMR (600 MHz, DMSO-*d*<sub>6</sub>) δ 11.56 (s, 1H), 8.52 (s, 1H), 8.22 (s, 1H), 7.96–7.74 (m, 1H), 7.69 (dd, *J* = 4.8, 8.5 Hz, 1H), 7.24–7.04 (m, 2H), 7.01–6.74 (m, 1H), 3.60 (dd, *J* = 6.7, 13.5 Hz, 2H), 1.72–1.56 (m, 2H), 1.47–1.30 (m, 2H), 0.91 (t, *J* = 7.4 Hz, 3H).

**1-[[2(S)-3,3-Dimethylbutan-2-yl]amino]-7-(1-methyl-1*H*-pyrazol-4-yl)-5*H*-pyrido[4,3-*b*]indole-4-carboxamide (**42**).**

**Step 1.** To **10b** (400 mg, 1.27 mmol) was added (*S*)-3,3-dimethyl-2-butanamine (10 mL, 76.0 mmol). The mixture was heated at 150 °C for 72 h, cooled to room temperature, and treated with water. The aqueous mixture was extracted with ethyl acetate (3×). The combined organic layers were dried with magnesium sulfate, filtered, and concentrated under reduced pressure. The residue was purified by chromatography on silica gel to afford 4-bromo-7-chloro-*N*-[(2*S*)-3,3-dimethylbutan-2-yl]-5*H*-pyrido[4,3-*b*]indol-1-amine (150 mg, 0.39 mmol, 31% yield) as a brown solid. LRMS (ESI) calcd for (C<sub>17</sub>H<sub>20</sub>BrClN<sub>3</sub>) [M + H]<sup>+</sup> 380.0, found 380.0. <sup>1</sup>H NMR (600 MHz, DMSO-*d*<sub>6</sub>) δ 11.86 (s, 1H), 8.14 (d, *J* = 8.5 Hz, 1H), 7.99 (s, 1H), 7.53 (d, *J* = 1.9 Hz, 1H), 7.29 (dd, *J* = 1.9, 8.3 Hz, 1H), 5.66–5.55 (m, 1H), 4.49–4.43 (m, 1H), 1.17 (d, *J* = 6.8 Hz, 3H), 0.95 (s, 9H).

**Step 2.** To 4-bromo-7-chloro-*N*-[(2*S*)-3,3-dimethylbutan-2-yl]-5*H*-pyrido[4,3-*b*]indol-1-amine (150 mg, 0.394 mmol) in NMP (3.94 mL) was added copper(I) cyanide (88 mg, 0.985 mmol). The reaction mixture was irradiated in the microwave at 225 °C for 1 h. The solution was cooled to room temperature, diluted with ethyl acetate, and washed with water. The organic layer was dried with magnesium sulfate, filtered, and concentrated under reduced pressure. The residue was purified by chromatography on silica gel to afford 7-chloro-1-[[2(*S*)-3,3-dimethylbutan-2-yl]amino]-5*H*-pyrido[4,3-*b*]indole-4-carbonitrile (21 mg, 0.06 mmol, 16% yield) as a brown solid. LRMS (ESI) calcd for (C<sub>18</sub>H<sub>20</sub>ClN<sub>4</sub>) [M + H]<sup>+</sup> 327.1, found 327.0. <sup>1</sup>H NMR (600 MHz, DMSO-*d*<sub>6</sub>) δ 12.47 (s, 1H), 8.39 (s, 1H), 8.24 (d, *J* = 8.5 Hz, 1H), 7.52 (d, *J* = 1.9 Hz, 1H), 7.32 (dd, *J* = 2.0, 8.4 Hz, 1H), 6.33 (d, *J* = 9.6 Hz, 1H), 4.63 (dd, *J* = 6.9, 9.5 Hz, 1H), 1.21 (d, *J* = 6.9 Hz, 3H), 0.94 (s, 9H).

**Step 3.** To a mixture of 7-chloro-1-[[2(*S*)-3,3-dimethylbutan-2-yl]amino]-5*H*-pyrido[4,3-*b*]indole-4-carbonitrile (21 mg, 0.064 mmol) and potassium carbonate (22 mg, 0.161 mmol) in DMSO (0.86 mL) was added hydrogen peroxide (30% solution in water, 0.033 mL, 0.321 mmol). The reaction mixture was stirred at 70 °C for 16 h. The mixture was cooled to room temperature and treated with water. The precipitate was filtered and dried to afford 7-chloro-1-[[2(*S*)-3,3-dimethylbutan-2-yl]amino]-5*H*-pyrido[4,3-*b*]indole-4-carboxamide (19 mg, 0.06 mmol, 86%) as a white solid. LRMS (ESI) calcd for (C<sub>18</sub>H<sub>22</sub>ClN<sub>4</sub>O) [M + H]<sup>+</sup> 345.1, found 345.1. <sup>1</sup>H NMR (600 MHz, DMSO-*d*<sub>6</sub>) δ 11.96 (s, 1H), 8.47 (s, 1H), 8.16 (d, *J* = 8.4 Hz, 1H), 7.99 (s, 1H), 7.80 (s, 1H), 7.40 (s,

1H), 7.29 (d, *J* = 8.4 Hz, 1H), 4.57–4.37 (m, 1H), 1.24 (d, *J* = 6.0 Hz, 3H), 0.96 (s, 9H).

**Step 4.** To 7-chloro-1-[[2(*S*)-3,3-dimethylbutan-2-yl]amino]-5*H*-pyrido[4,3-*b*]indole-4-carboxamide (14 mg, 0.041 mmol), Pd<sub>2</sub>(dba)<sub>3</sub> (3.7 mg, 0.004 mmol), tricyclohexylphosphine (2.9 mg, 0.010 mmol), and tribasic potassium phosphate (1.27 M in water, 0.389 mL, 0.50 mmol) in dioxane (0.83 mL) was added 1-methyl-4-(4,4,5,5-tetra-methyl-1,3,2-dioxaborolan-2-yl)-1*H*-pyrazole (13 mg, 0.061 mmol). The reaction solution was purged with nitrogen gas for 5 min and heated to 100 °C for 16 h. The solution was cooled to room temperature, diluted with ethyl acetate, and washed with water (3×). The organic layer was dried with magnesium sulfate, filtered, and concentrated. The residue was purified by chromatography on silica gel to afford **42** (4 mg, 0.01 mmol, 25% yield) as an off white solid. LRMS (ESI) calcd for (C<sub>22</sub>H<sub>27</sub>N<sub>6</sub>O) [M + H]<sup>+</sup> 391.2, found 391.2. <sup>1</sup>H NMR (600 MHz, DMSO-*d*<sub>6</sub>) δ 11.43 (s, 1H), 8.48 (s, 1H), 8.08 (s, 1H), 8.03 (d, *J* = 8.2 Hz, 1H), 7.87 (br, s, 1H), 7.85 (s, 1H), 7.81 (s, 1H), 7.44 (d, *J* = 8.1 Hz, 1H), 7.13 (br, s, 1H), 5.72 (s, 1H), 4.63–4.53 (m, 1H), 3.87 (s, 3H), 1.20 (d, *J* = 6.7 Hz, 3H), 0.97 (s, 9H).

**(1*S*)-1-Cyclopropylethanaminium Chloride.** **Step 1.** To a stirred solution of cyclopropanecarboxaldehyde (24.9 g, 355 mmol) in dichloromethane (355 mL) were added (*S*)-2-methyl-2-propanesulfonamide (**13a**, 21.5 g, 177 mmol), magnesium sulfate (107 g, 887 mmol), and PPTS (2.23 g, 8.87 mmol). The reaction mixture was left to stir overnight, filtered through a fritted funnel, concentrated, and purified by chromatography to provide **14a** (28.4 g, 164 mmol, 92% yield) as a colorless oil. LRMS (ESI) calcd for (C<sub>8</sub>H<sub>16</sub>NOS) [M + H]<sup>+</sup> 174.1, found 174.1. <sup>1</sup>H NMR (600 MHz, CDCl<sub>3</sub>) δ 7.42 (d, *J* = 8.0 Hz, 1H), 1.99–1.93 (m, 1H), 1.16 (s, 9H), 1.09–1.04 (m, 2H), 0.96–0.92 (m, 2H).

**Step 2.** To a stirred solution of **14a** (1.0 g, 5.8 mmol) in dichloromethane (36 mL) was added MeMgBr (3.0 M in ether, 4.6 mL, 13.8 mmol) slowly at –52 °C in a cryobath. The reaction mixture was left to stir at –48 °C for 3 h and allowed to warm to room temperature overnight. The mixture was treated with saturated NH<sub>4</sub>Cl solution and extracted with ethyl acetate (3×). The combined organics were washed with brine, dried over sodium sulfate, concentrated, and purified by flash chromatography to afford *N*-[(1*S*)-1-cyclopropylethyl]-(*S*)-2-methylpropane-2-sulfonamide (1.0 g, 5.3 mmol, 91% yield). LRMS (ESI) calcd for (C<sub>9</sub>H<sub>20</sub>NOS) [M + H]<sup>+</sup> 190.1, found 190.1. <sup>1</sup>H NMR (600 MHz, CDCl<sub>3</sub>) δ 3.06 (d, *J* = 4.1 Hz, 1H), 2.73 (m, 1H), 1.32 (d, *J* = 6.8 Hz, 3H), 1.21 (s, 9H), 0.80 (m, 1H), 0.55 (m, 1H), 0.47 (m, 1H), 0.37 (m, 1H), 0.17 (m, 1H).

**Step 3.** To a stirred solution of *N*-[(1*S*)-1-cyclopropylethyl]-(*S*)-2-methylpropane-2-sulfonamide (1.0 g, 5.3 mmol) in MeOH (2.7 mL) was added HCl in dioxane (4*N*, 2.75 mL, 11.0 mmol). The reaction mixture was left to stir for 30 min and concentrated in vacuo to half of the volume. Ether was added to the mixture, and the white precipitate was collected by filtration to afford (1*S*)-1-cyclopropylethanaminium chloride (615 mg, 5.06 mmol, 92% yield). <sup>1</sup>H NMR (600 MHz, DMSO-*d*<sub>6</sub>) δ 8.00 (brs, 3H), 2.48 (m, 1H), 1.24 (d, *J* = 6.7 Hz, 3H), 0.91 (m, 1H), 0.51 (m, 2H), 0.42 (m, 1H), 0.28 (m, 1H).

**(1*R*)-1-Cyclopropyl-2,2,2-trifluoroethanaminium Chloride.** **Step 1.** To a stirred solution of **14a** (10.0 g, 57.7 mmol) in THF (290 mL) was added TMAF (6.45 g, 69.3 mmol). The reaction mixture was purged with N<sub>2</sub>. The solution was cooled to –55 °C, and a solution of TMSCF<sub>3</sub> (13.53 mL, 87.0 mmol) in THF (430 mL) was added via syringe slowly. The mixture was stirred at –55 °C until the reaction was complete. The solution was warmed to –10 °C and treated with saturated NH<sub>4</sub>Cl (10 mL). The aqueous layer was extracted with ethyl acetate (3×), and the combined organics were dried with magnesium sulfate, filtered, and concentrated under reduced pressure. The diastereomers were separated by flash chromatography to afford *N*-[(1*R*)-1-cyclopropyl-2,2,2-trifluoroethyl]-(*S*)-2-methylpropane-2-sulfonamide

(10.0 g, 41.1 mmol, 71% yield) and *N*-[(1*S*)-1-cyclopropyl-2,2,2-trifluoroethyl]-(*S*)-2-methylpropane-2-sulfinamide (960 mg, 3.95 mmol, 7% yield) as white solids. *N*-[(1*R*)-1-cyclopropyl-2,2,2-trifluoroethyl]-(*S*)-2-methylpropane-2-sulfinamide:  $^1\text{H NMR}$  (600 MHz,  $\text{CDCl}_3$ )  $\delta$  3.32 (d,  $J = 5.7$  Hz, 1H), 2.94–2.87 (m, 1H), 1.22 (s, 9H), 1.10–1.01 (m, 1H), 0.82–0.76 (m, 1H), 0.72–0.66 (m, 1H), 0.66–0.60 (m, 1H), 0.52–0.47 (m, 1H). *N*-[(1*S*)-1-cyclopropyl-2,2,2-trifluoroethyl]-(*S*)-2-methylpropane-2-sulfinamide:  $^1\text{H NMR}$  (600 MHz,  $\text{CDCl}_3$ )  $\delta$  3.62 (d,  $J = 5.2$  Hz, 1H), 3.02–2.94 (m, 1H), 1.24 (s, 9H), 1.10–0.98 (m, 1H), 0.82–0.78 (m, 2H), 0.72–0.66 (m, 1H), 0.66–0.60 (m, 1H), 0.51–0.46 (m, 1H).

**Step 2.** *N*-[(1*R*)-1-cyclopropyl-2,2,2-trifluoroethyl]-(*S*)-2-methylpropane-2-sulfinamide (16.55 g, 68.0 mmol) was dissolved in MeOH (34 mL), and 4 M HCl in dioxane (34.0 mL, 136 mmol) was added. The reaction mixture was allowed to stir for 30 min and concentrated to half the volume. Ether was added to the mixture, and the resultant precipitate was filtered to afford (1*R*)-1-cyclopropyl-2,2,2-trifluoroethanaminium chloride (10.8 g, 61.5 mmol, 90% yield) as a white solid.  $^1\text{H NMR}$  (500 MHz,  $\text{D}_2\text{O}$ )  $\delta$  3.44 (m, 1H), 1.27 (m, 1H), 0.85–0.98 (m, 2H), 0.75 (m, 1H), 0.58 (m, 1H).

**1-[[1*S*]-1-cyclopropylethyl]amino]-7-(1-methyl-1*H*-pyrazol-4-yl)-5*H*-pyrido[4,3-*b*]indole-4-carboxamide (48).** **Step 1.** A mixture of **6b** (150 mg, 0.572 mmol), (1*S*)-1-cyclopropylethanaminium chloride (209 mg, 1.72 mmol), and diisopropylethylamine (400  $\mu\text{L}$ , 2.29 mmol) in dioxane (7.2 mL) was heated to 140 °C for 3 days. The mixture was diluted with ethyl acetate and washed with 50% brine. The organic layer was dried over sodium sulfate, concentrated, and purified by flash chromatography to afford 7-chloro-1-[[1*S*]-1-cyclopropylethyl]amino]-5*H*-pyrido[4,3-*b*]indole-4-carbonitrile (133 mg, 0.43 mmol, 75% yield). LRMS (ESI) calcd for ( $\text{C}_{17}\text{H}_{16}\text{ClN}_4$ ) [M + H] $^+$  311.1, found 311.0.  $^1\text{H NMR}$  (600 MHz,  $\text{CDCl}_3$ )  $\delta$  8.98 (brs, 1H), 8.38 (s, 1H), 7.70 (d,  $J = 8.5$  Hz, 1H), 7.56 (d,  $J = 1.8$  Hz, 1H), 7.36 (dd,  $J = 1.8, 8.2$  Hz, 1H), 5.33 (d,  $J = 7.3$  Hz, 1H), 3.98 (m, 1H), 1.43 (d,  $J = 6.5$  Hz, 3H), 1.09 (m, 1H), 0.63 (m, 1H), 0.56 (m, 1H), 0.46 (m, 1H), 0.39 (m, 1H).

**Step 2.** 7-Chloro-1-[[1*S*]-1-cyclopropylethyl]amino]-5*H*-pyrido[4,3-*b*]indole-4-carbonitrile (2.10 g, 6.76 mmol) and potassium carbonate (4.67 g, 33.8 mmol) were placed in a flask. DMSO (67.6 mL) and hydrogen peroxide (30%, 6.91 mL, 67.6 mmol) were added, and the solution was heated at 85 °C overnight. The reaction mixture was cooled to room temperature, diluted with ethyl acetate, and washed with water and brine. The organic layer was dried with magnesium sulfate, concentrated, and purified by HPLC to afford 7-chloro-1-[[1*S*]-1-cyclopropylethyl]amino]-5*H*-pyrido[4,3-*b*]indole-4-carboxamide (1.87 g, 5.69 mmol, 84% yield). LRMS (ESI) calcd for ( $\text{C}_{17}\text{H}_{18}\text{ClN}_4\text{O}$ ) [M + H] $^+$  329.1, found 329.1.  $^1\text{H NMR}$  (600 MHz,  $\text{DMSO}-d_6$ )  $\delta$  11.67 (s, 1H), 8.53 (s, 1H), 8.36 (d,  $J = 8.5$  Hz, 1H), 7.87 (brs, 1H), 7.78 (d,  $J = 2.0$  Hz, 1H), 7.26 (dd,  $J = 2.1, 8.5$  Hz, 1H), 7.19 (brs, 1H), 6.50 (d,  $J = 8.3$  Hz, 1H), 4.00 (m, 1H), 1.36 (d,  $J = 6.7$  Hz, 3H), 1.28 (m, 1H), 0.49 (m, 1H), 0.40 (m, 1H), 0.36 (m, 1H), 0.26 (m, 1H).

**Step 3.** A mixture of 7-chloro-1-[[1*S*]-1-cyclopropylethyl]amino]-5*H*-pyrido[4,3-*b*]indole-4-carboxamide (45 mg, 0.14 mmol), 1-methyl-4-(4,4,5,5-tetramethyl-1,3,2-dioxaborolan-2-yl)-1*H*-pyrazole (34.2 mg, 0.164 mmol),  $\text{Pd}_2(\text{dba})_3$  (12.5 mg, 0.014 mmol), tricyclohexylphosphine (9.60 mg, 0.034 mmol), and potassium phosphate tribasic (1.27 M, 367  $\mu\text{L}$ , 0.466 mmol) in dioxane (2.7 mL) was purged with nitrogen for 10 min and heated to 100 °C for 3 h. The mixture was cooled to room temperature, concentrated, and purified by flash chromatography to afford **48** (49 mg, 0.13 mmol, 96%). LRMS (ESI) calcd for ( $\text{C}_{21}\text{H}_{23}\text{N}_6\text{O}$ ) [M + H] $^+$  375.2, found 375.2.  $^1\text{H NMR}$  (600 MHz,  $\text{DMSO}-d_6$ )  $\delta$  11.43 (s, 1H), 8.48 (s, 1H), 8.29 (d,  $J = 8.2$  Hz, 1H), 8.11 (s, 1H), 7.87 (d,  $J = 1.4$  Hz, 1H), 7.85 (brs, 1H), 7.32 (s, 1H), 7.44 (dd,  $J = 8.2, 1.4$  Hz, 1H), 7.13 (brs, 1H), 6.36 (d,  $J = 8.5$  Hz, 1H), 4.02 (m, 1H), 3.90 (s, 3H), 1.37 (d,  $J = 6.4$  Hz, 3H), 1.29 (m, 1H), 0.50 (m, 1H), 0.41 (m, 1H), 0.37 (m, 1H), 0.27 (m, 1H).

**1-[[1*R*]-1-cyclopropyl-2,2,2-trifluoroethyl]amino]-7-(1-methyl-1*H*-pyrazol-4-yl)-5*H*-pyrido[4,3-*b*]indole-4-carboxamide (52).** **Step 1.** To a stirred slurry of **6b** (2.5 g, 9.54 mmol) in dioxane (70 mL) in a pressure vessel were added dicyclopropylmethanaminium chloride (5.07 g, 34.3 mmol) and diisopropylethylamine (7.66 mL, 43.9 mmol). The reaction mixture was heated to 145 °C for 3 days, treated with additional dicyclopropylmethanaminium chloride (2.0 g, 13.5 mmol) and diisopropylethylamine (3.0 mL, 17 mmol), and heated to 145 °C for 4 days. The reaction mixture was cooled to room temperature and concentrated. The residue was diluted with ethyl acetate and saturated  $\text{NaHCO}_3$  solution. The aqueous layer was extracted with ethyl acetate (3 $\times$ ). The combined organics were washed with brine, dried over sodium sulfate, concentrated, and purified by flash chromatography to afford 7-chloro-1-[[1*R*]-1-cyclopropyl-2,2,2-trifluoroethyl]amino]-5*H*-pyrido[4,3-*b*]indole-4-carbonitrile (2.30 g, 6.82 mmol, 72% yield). LRMS (ESI) calcd for ( $\text{C}_{19}\text{H}_{18}\text{ClN}_4$ ) [M + H] $^+$  337.1, found 337.1.  $^1\text{H NMR}$  (600 MHz,  $\text{DMSO}-d_6$ )  $\delta$  12.45 (brs, 1H), 8.52 (d,  $J = 8.5$  Hz, 1H), 8.33 (s, 1H), 7.54 (d,  $J = 2.1$  Hz, 1H), 7.36 (dd,  $J = 2.1, 8.5$  Hz, 1H), 7.05 (d,  $J = 8.8$  Hz, 1H), 3.54 (m, 1H), 1.37 (m, 2H), 0.53 (m, 2H), 0.38 (m, 2H), 0.35 (m, 2H), 0.29 (m, 2H).

**Step 2.** To a stirred solution of 7-chloro-1-[[1*R*]-1-cyclopropyl-2,2,2-trifluoroethyl]amino]-5*H*-pyrido[4,3-*b*]indole-4-carbonitrile (2.47 g, 7.33 mmol) in DMSO (73 mL) were added potassium carbonate (6.08 g, 44.0 mmol) and 30%  $\text{H}_2\text{O}_2$  (8.99 mL, 88.0 mmol). The reaction mixture was heated to 85 °C for 5 h, cooled to room temperature, and diluted with ethyl acetate and water. The mixture was extracted with ethyl acetate (3 $\times$ ). The combined organics were washed with brine, dried over sodium sulfate, concentrated, and purified by flash chromatography to afford 7-chloro-1-[[1*R*]-1-cyclopropyl-2,2,2-trifluoroethyl]amino]-5*H*-pyrido[4,3-*b*]indole-4-carboxamide (2.59 g, 7.30 mmol, 100% yield). LRMS (ESI) calcd for ( $\text{C}_{19}\text{H}_{20}\text{ClN}_4\text{O}$ ) [M + H] $^+$  355.1, found 355.1.  $^1\text{H NMR}$  (500 MHz,  $\text{DMSO}-d_6$ )  $\delta$  11.67 (s, 1H), 8.47 (s, 1H), 8.41 (d,  $J = 8.2$  Hz, 1H), 7.83 (brs, 1H), 7.78 (s, 1H), 7.26 (d,  $J = 8.5$  Hz, 1H), 7.18 (brs, 1H), 6.57 (d,  $J = 8.5$  Hz, 1H), 3.61 (q,  $J = 8.5$  Hz, 1H), 1.35 (m, 2H), 0.51 (m, 2H), 0.32–0.40 (m, 6H).

**Step 3.** A mixture of 7-chloro-1-[[1*R*]-1-cyclopropyl-2,2,2-trifluoroethyl]amino]-5*H*-pyrido[4,3-*b*]indole-4-carboxamide (53 mg, 0.15 mmol), 1-methyl-4-(4,4,5,5-tetramethyl-1,3,2-dioxaborolan-2-yl)-1*H*-pyrazole (40.4 mg, 0.194 mmol),  $\text{Pd}_2(\text{dba})_3$  (13.7 mg, 0.015 mmol), tricyclohexylphosphine (10.5 mg, 0.037 mmol), and potassium phosphate tribasic (1.27 M, 400  $\mu\text{L}$ , 0.51 mmol) in dioxane (3 mL) was purged with nitrogen for 10 min and heated to 100 °C for 3 h. The mixture was cooled to room temperature, concentrated, and purified by flash chromatography to afford **52** (43 mg, 0.11 mmol, 72% yield). LRMS (ESI) calcd for ( $\text{C}_{23}\text{H}_{25}\text{N}_6\text{O}$ ) [M + H] $^+$  401.2, found 401.2.  $^1\text{H NMR}$  (600 MHz,  $\text{DMSO}-d_6$ )  $\delta$  11.43 (s, 1H), 8.43 (s, 1H), 8.33 (d,  $J = 8.2$  Hz, 1H), 8.12 (s, 1H), 7.87 (d,  $J = 1.1$  Hz, 1H), 7.84 (s, 1H), 7.81 (brs, 1H), 7.45 (dd,  $J = 1.7, 8.0$  Hz, 1H), 7.12 (brs, 1H), 6.42 (d,  $J = 8.5$  Hz, 1H), 3.90 (s, 3H), 3.63 (m, 1H), 1.37 (m, 2H), 0.51 (m, 2H), 0.34–0.38 (m, 6H).

**1-[[1*R*]-1-cyclopropyl-2,2,2-trifluoroethyl]amino]-7-(1-methyl-1*H*-pyrazol-4-yl)-5*H*-pyrido[4,3-*b*]indole-4-carboxamide (53).** **Step 1.** To **6b** (5.0 g, 19.1 mmol),  $\text{Pd}_2(\text{dba})_3$  (873 mg, 0.95 mmol), BINAP (1.78 g, 2.86 mmol), and sodium *tert*-butoxide (9.17 g, 95.0 mmol) in DME (125 mL) was added (1*R*)-1-cyclopropyl-2,2,2-trifluoroethanaminium chloride (5.02 g, 28.6 mmol). The slurry was purged with nitrogen gas for 15 min. The mixture was heated at 85 °C for 16 h. The mixture was cooled to room temperature, diluted with ethyl acetate, and washed with water (2 $\times$ ) and brine. The organic layer was dried with magnesium sulfate, filtered, and concentrated under reduced pressure. The residue was purified by chromatography on silica gel to afford 7-chloro-1-[[1*R*]-1-cyclopropyl-2,2,2-trifluoroethyl]amino]-5*H*-pyrido[4,3-*b*]indole-4-carbonitrile (4.24 g, 11.62 mmol, 61% yield) as an off white solid. LRMS (ESI) calcd for ( $\text{C}_{17}\text{H}_{13}\text{ClF}_3\text{N}_4$ ) [M + H] $^+$  365.1, found 365.0.  $^1\text{H NMR}$  (600 MHz,  $\text{DMSO}-d_6$ )  $\delta$  12.62

(s, 1H), 8.56 (d,  $J = 8.5$  Hz, 1H), 8.40 (s, 1H), 7.54 (d,  $J = 1.9$  Hz, 1H), 7.46 (d,  $J = 8.8$  Hz, 1H), 7.36 (dd,  $J = 1.9, 8.5$  Hz, 1H), 4.81–4.73 (m, 1H), 1.59–1.52 (m, 1H), 0.76–0.70 (m, 1H), 0.64–0.58 (m, 1H), 0.54–0.47 (m, 1H), 0.29–0.24 (m, 1H).

**Step 2.** To 7-chloro-1-[[*(1R)*-1-cyclopropyl-2,2,2-trifluoroethyl]-amino]-5*H*-pyrido[4,3-*b*]indole-4-carbonitrile (4.20 g, 11.51 mmol) and potassium carbonate (7.96 g, 57.6 mmol) in DMSO (230 mL) was added hydrogen peroxide (30% solution in water, 11.76 mL, 115 mmol). The mixture was heated to 80 °C for 4 h. The solution was cooled to room temperature and diluted with ethyl acetate. The organic layer was washed with water (3×) and brine. The organic layer was dried with magnesium sulfate, filtered, and concentrated under reduced pressure. The residue was purified by chromatography on silica gel to afford 7-chloro-1-[[*(1R)*-1-cyclopropyl-2,2,2-trifluoroethyl]amino]-5*H*-pyrido[4,3-*b*]indole-4-carboxamide (3.22 g, 8.41 mmol, 73% yield) as a yellow solid. LRMS (ESI) calcd for (C<sub>17</sub>H<sub>15</sub>ClF<sub>3</sub>N<sub>4</sub>O) [M + H]<sup>+</sup> 383.1, found 383.0. <sup>1</sup>H NMR (600 MHz, DMSO-*d*<sub>6</sub>) δ 11.77 (s, 1H), 8.50 (s, 1H), 8.47 (d,  $J = 8.4$  Hz, 1H), 7.93 (br, s, 1H), 7.77 (s, 1H), 7.29 (br, s, 1H), 7.26 (d,  $J = 8.4$  Hz, 1H), 7.04 (d,  $J = 8.8$  Hz, 1H), 4.87–4.77 (m, 1H), 1.58–1.51 (m, 1H), 0.74–0.68 (m, 1H), 0.64–0.57 (m, 1H), 0.53–0.46 (m, 1H), 0.32–0.26 (m, 1H).

**Step 3.** To 7-chloro-1-[[*(1R)*-1-cyclopropyl-2,2,2-trifluoroethyl]-amino]-5*H*-pyrido[4,3-*b*]indole-4-carboxamide (51 mg, 0.13 mmol), Pd<sub>2</sub>(dba)<sub>3</sub> (12 mg, 0.013 mmol), tricyclohexylphosphine (9.3 mg, 0.033 mmol), and tribasic potassium phosphate (1.27 M in water, 0.36 mL, 0.45 mmol) in dioxane (2.7 mL) was added 1-methyl-4-(4,4,5,5-tetramethyl-1,3,2-dioxaborolan-2-yl)-1*H*-pyrazole (55 mg, 0.27 mmol). The reaction solution was purged with nitrogen gas for 5 min and heated to 100 °C for 16 h. The solution was cooled to room temperature, diluted with ethyl acetate, and washed with water (3×). The organic layer was dried with magnesium sulfate, filtered, and concentrated. The residue was purified by chromatography on silica gel to afford 53 (57 mg, 0.13 mmol, 100%) as a yellow solid. LRMS (ESI) calcd for (C<sub>21</sub>H<sub>20</sub>F<sub>3</sub>N<sub>6</sub>O) [M + H]<sup>+</sup> 429.2, found 429.1. <sup>1</sup>H NMR (600 MHz, DMSO-*d*<sub>6</sub>) δ 11.54 (s, 1H), 8.46 (s, 1H), 8.39 (d,  $J = 8.3$  Hz, 1H), 8.10 (s, 1H), 7.90 (br, s, 1H), 7.85 (s, 1H), 7.81 (s, 1H), 7.44 (d,  $J = 8.2$  Hz, 1H), 7.24 (br, s, 1H), 6.89 (d,  $J = 8.8$  Hz, 1H), 4.86–4.79 (m, 1H), 3.86 (s, 3H), 1.78–1.73 (m, 1H), 0.75–0.69 (m, 1H), 0.63–0.58 (m, 1H), 0.53–0.47 (m, 1H), 0.34–0.27 (m, 1H).

**7-(2-Aminopyrimidin-5-yl)-1-[(dicyclopropylmethyl)amino]-5*H*-pyrido[4,3-*b*]indole-4-carboxamide (60).** A mixture of 7-chloro-1-[[*(dicyclopropylmethyl)amino*]-5*H*-pyrido[4,3-*b*]indole-4-carboxamide (70 mg, 0.20 mmol), 5-(4,4,5,5-tetramethyl-1,3,2-dioxaborolan-2-yl)-pyrimidin-2-ylamine (61 mg, 0.28 mmol), Pd<sub>2</sub>(dba)<sub>3</sub> (18 mg, 0.02 mmol), tricyclohexylphosphine (14 mg, 0.05 mmol), and K<sub>3</sub>PO<sub>4</sub> (1.27 M in water, 0.53 mL, 0.67 mmol) in dioxane (4 mL) was purged with nitrogen for 5 min, heated to 100 °C for 3 h, cooled to room temperature, and concentrated. The residue was purified by flash chromatography to afford 60 (60 mg, 0.15 mmol, 74% yield) as a white solid. LRMS (ESI) calcd for (C<sub>23</sub>H<sub>24</sub>N<sub>7</sub>O) [M + H]<sup>+</sup>, 414.2, found 414.1. <sup>1</sup>H NMR (500 MHz, DMSO-*d*<sub>6</sub>) δ 11.50 (s, 1H), 8.61 (s, 2H), 8.45 (s, 1H), 8.43 (d,  $J = 8.2$  Hz, 1H), 7.92 (s, 1H), 7.83 (brs, 1H), 7.49 (d,  $J = 8.2$  Hz, 1H), 7.18 (brs, 1H), 6.78 (s, 2H), 6.51 (d,  $J = 8.8$  Hz, 1H), 3.63 (q,  $J = 8.5$  Hz, 1H), 1.38 (m, 2H), 0.51 (m, 2H), 0.36 (m, 6H).

**7-(2-Aminopyrimidin-5-yl)-1-[[*(1R)*-1-cyclopropyl-2,2,2-trifluoroethyl]amino]-5*H*-pyrido[4,3-*b*]indole-4-carboxamide (65).** To 7-chloro-1-[[*(1R)*-1-cyclopropyl-2,2,2-trifluoroethyl]-amino]-5*H*-pyrido[4,3-*b*]indole-4-carboxamide (8.36 g, 21.84 mmol), Pd<sub>2</sub>(dba)<sub>3</sub> (2.0 g, 2.18 mmol), tricyclohexylphosphine (1.53 g, 5.46 mmol), and tribasic potassium phosphate (1.27 M in water, 59.2 mL, 74.0 mmol) in dioxane (437 mL) was added 5-(4,4,5,5-tetramethyl-1,3,2-dioxaborolan-2-yl)pyrimidin-2-amine (7.73 g, 34.9 mmol). The reaction solution was purged with nitrogen gas for 15 min and heated to 100 °C for 2 h. The solution was cooled to room temperature, diluted

with ethyl acetate, and washed with water (3×). The organic layer was dried with magnesium sulfate, filtered, and concentrated. The residue was purified by chromatography on silica gel to afford 65 (8.20 g, 18.58 mmol, 85% yield) as a yellow solid. LRMS (ESI) calcd for (C<sub>21</sub>H<sub>19</sub>F<sub>3</sub>N<sub>7</sub>O) [M + H]<sup>+</sup> 442.2, found 442.1. <sup>1</sup>H NMR (500 MHz, DMSO-*d*<sub>6</sub>) δ 11.63 (s, 1H), 8.61 (s, 2H), 8.51 (d,  $J = 8.4$  Hz, 1H), 8.50 (s, 1H), 7.96 (br, s, 1H), 7.92 (s, 1H), 7.51 (d,  $J = 8.2$  Hz, 1H), 7.26 (br, s, 1H), 7.00 (d,  $J = 8.8$  Hz, 1H), 6.77 (s, 2H), 4.95–4.72 (m, 1H), 1.64–1.49 (m, 1H), 0.78–0.70 (m, 1H), 0.66–0.58 (m, 1H), 0.57–0.49 (m, 1H), 0.36–0.29 (m, 1H).

**In Vitro Kinase Assays.** JAK1, JAK2, and JAK3 kinase activity assays were performed as described previously<sup>35</sup> using HTRF detection technology and the peptide substrate amino hexanoyl biotin-EQDE-PEGDYFEWLE-NH<sub>2</sub>. Each mixture was incubated between 60 and 80 min at room temperature. Final conditions were as follows: JAK1, 400 pM enzyme, Hepes, pH 7.5, 10 mM MgCl<sub>2</sub>, 0.01% Brij-35, 1 mM EGTA, 0.1 mg/mL BSA, 2 mM DTT, 2 μM peptide substrate, 25 μM MgATP, 5% DMSO, and the desired concentration of subject compound; JAK2, 25 pM enzyme (JH1, JH1-JH2<sup>wt</sup>, JH1-JH2<sup>V617F</sup> domains), 2 μM peptide substrate, 15 μM MgATP, 5 mM MgCl<sub>2</sub>, 100 mM NaCl, 2 mM DTT, 0.1 mg/mL BSA, 50 mM Tris (pH 7.4), 5% DMSO, and the desired concentration of subject compound; JAK3, 250 pM enzyme, 50 mM Hepes, pH 7.5, 10 mM MgCl<sub>2</sub>, 0.01% Brij-35, 1 mM EGTA, 0.1 mg/mL BSA, 2 mM DTT, 2.0 μM peptide substrate, 25 μM MgATP, 5% DMSO, and the desired concentration of subject compound. Kinase profiling was conducted by Millipore (Billerica, MA).

**Cellular Assays.** Measurement of pSTAT5 in cells was performed essentially as described previously<sup>35</sup> using an AlphaScreen SureFire (Perkin-Elmer and TGR Biosciences) assay. AlphaScreen SureFire p-STAT5 assay uses both biotinylated anti-phospho-STAT5 antibody, which is captured by streptavidin-coated donor beads, and antitotal STAT5 antibody, which is captured by protein A conjugated acceptor beads. The irf1-*bla* HEL CellSensor cell line was created by transducing parental HEL 92.1.7 cells (ATCC) with the pLenti-*bsd*/irf1-*bla* CellSensor vector. When both antibodies bind to phospho-STAT5 proteins released from HEL irf1-*bla* cells, the donor and acceptor beads are brought into proximity (≤200 nm) and a cascade of chemical reactions is initiated to produce a greatly amplified signal. Upon laser excitation, a photosensitizer in the donor bead converts ambient oxygen to a more excited singlet state. The singlet state oxygen molecules diffuse across to react with a chemiluminescer in the acceptor bead that further activates fluorophores contained within the same bead. The fluorophores subsequently emit light at 520–620 nm. The emitted light intensity is directly proportional to the amount of phospho-STAT5 proteins released from HEL irf1-*bla* cells.

**Crystallography.** Jak2 protein was mixed with CMP and concentrated to 3.1 mg/mL in a buffer containing 20 mM Tris, pH 8.5, 250 mM NaCl, 0.5 mM EDTA, 2 mM DTT. Crystals were obtained by mixing the protein/inhibitor complex in a 1:1 ratio with reservoir solution containing 0.1 M Hepes, pH 7.5, 33.5% PEG3350, 100 ammonium sulfate, using the hanging drop technique. Streak seeding was performed to improve crystal size. Crystals were cryoprotected using the reservoir solution, with addition of 10% PEG400, by immediate immersion into liquid nitrogen. Data were collected at the IMCA beamline (17-BM) at the Advanced Photon Source using X-ray of 1.00 Å wavelength and collected on a MAR165 detector. Data were processed using HKL2000,<sup>36</sup> and phases were determined by molecular replacement using Phaser<sup>37</sup> with an in-house Jak2 structure as the search model. The structure was iteratively rebuilt using Coot<sup>38</sup> and refined with Refmac.<sup>39</sup> Figures were prepared using PyMOL.

## ■ ASSOCIATED CONTENT

Supporting Information. Experimental procedures and LRMS and <sup>1</sup>H NMR data for compounds 3, 18, 19, 21–41,

43–47, 49–51, 54–59, 61–64; X-ray statistics for 38. This material is available free of charge via the Internet at <http://pubs.acs.org>.

#### Accession Codes

<sup>†</sup>PDB code for 38 is 3RVG.

### AUTHOR INFORMATION

#### Corresponding Author

\*Phone: 617-992-2012. E-mail: [jongwon\\_lim@merck.com](mailto:jongwon_lim@merck.com).

### ACKNOWLEDGMENT

We thank Michele Kubryk and Jeffrey Fritzen for preparation of key intermediates and Regina Black for purification of key intermediates.

### ABBREVIATIONS USED

ATP, adenosine triphosphate; AUC, area under the curve; CF<sub>3</sub>TMS, trimethyl(trifluoromethyl)silane; Cl<sub>p</sub>, plasma clearance; EPO, erythropoietin; ET, essential thrombocythemia; GM-CSF, granulocyte-macrophage colony stimulating factor; hERG, human ether-a-go-go-related gene; IL, interleukin; iv, intravenous; JAK, Janus kinase; MPD, myeloproliferative disorder; NBS, N-bromosuccinimide; PMF, primary myelofibrosis; PK, pharmacokinetic; PV, polycythemia vera Q<sub>hep</sub>, hepatic blood flow; SAR, structure–activity relationship; STAT, signal transducer and activator of transcription; TMAF, tetramethylammonium fluoride; TPO, thrombopoietin; V<sub>d</sub>, volume of distribution

### REFERENCES

- (1) Ihle, J. N.; Kerr, I. M. Jaks and Stats in Signaling by the Cytokine Receptor Superfamily. *Trends Genet.* **1995**, *11*, 69–74.
- (2) Ihle, J. N. The Janus Protein Tyrosine Kinases in Hematopoietic Cytokine Signaling. *Semin. Immunol.* **1995**, *7*, 247–254.
- (3) Shuai, K.; Liu, B. Regulation of JAK–STAT Signalling in the Immune System. *Nat. Rev. Immunol.* **2003**, *3*, 900–911.
- (4) Yu, H.; Pardoll, D.; Jove, R. STATs in Cancer Inflammation and Immunity: A Leading Role for STAT3. *Nat. Rev. Cancer* **2009**, *9*, 798–809.
- (5) Valentino, L.; Pierre, J. JAK/STAT Signal Transduction: Regulators and Implication in Hematological Malignancies. *Biochem. Pharmacol.* **2006**, *71*, 713–721.
- (6) Baxter, E. J.; Scott, L. M.; Campbell, P. J.; East, C.; Fourouclas, N.; Swanton, S.; Vassiliou, G. S.; Bench, A. J.; Boyd, E. M.; Curtin, N.; Scott, M. A.; Erber, W. N.; Green, A. R. Acquired Mutation of the Tyrosine Kinase JAK2 in Human Myeloproliferative Disorders. *Lancet* **2005**, *365*, 1054–1061.
- (7) James, C.; Ugo, V.; Le Couedic, J. P.; Staerk, J.; Delhommeau, F.; Lacout, C.; Garcon, L.; Raslova, H.; Berger, R.; Bennaceur-Griscelli, A.; Villeval, J. L.; Constantinescu, S. N.; Casadevall, N.; Vainchenker, W. A Unique Clonal JAK2 Mutation Leading to Constitutive Signalling Causes Polycythemia Vera. *Nature* **2005**, *434*, 1144–1148.
- (8) Kralovics, R.; Passamonti, F.; Buser, A. S.; Teo, S.-S.; Tiedt, R.; Passweg, J. R.; Tichelli, A.; Cazzola, M.; Skoda, R. C. A Gain-of-Function Mutation of JAK2 in Myeloproliferative Disorders. *N. Engl. J. Med.* **2005**, *352*, 1779–1790.
- (9) Levine, R. L.; Wadleigh, M.; Cools, J.; Ebert, B. L.; Wernig, G.; Huntly, B. J. P.; Boggon, T. J.; Wlodarska, I.; Clark, J. J.; Moore, S.; Adelsperger, J.; Koo, S.; Lee, J. C.; Gabriel, S.; Mercher, T.; D'Andrea, A.; Froehling, S.; Doehner, K.; Marynen, P.; Vandenberghe, P.; Mesa, R. A.; Tefferi, A.; Griffin, J. D.; Eck, M. J.; Sellers, W. R.; Meyerson, M.; Golub, T. R.; Lee, S. J.; Gilliland, D. G. Activating Mutation in the Tyrosine

Kinase JAK2 in Polycythemia Vera, Essential Thrombocythemia, and Myeloid Metaplasia with Myelofibrosis. *Cancer Cell* **2005**, *7*, 387–397.

- (10) Zhao, R.; Xing, S.; Li, Z.; Fu, X.; Li, Q.; Krantz, S. B.; Zhao, Z. J. Identification of an Acquired JAK2 Mutation in Polycythemia Vera. *J. Biol. Chem.* **2005**, *280*, 22788–22792.

- (11) Bumm, T. G. P.; Elsea, C.; Corbin, A. S.; Loriaux, M.; Sherbenou, D.; Wood, L.; Deininger, J.; Silver, R. T.; Druker, B. J.; Deininger, M. W. N. Characterization of Murine JAK2V617F-Positive Myeloproliferative Disease. *Cancer Res.* **2006**, *66*, 11156–11165.

- (12) Lacout, C.; Pisani, D. F.; Tulliez, M.; Gachelin, F. M.; Vainchenker, W.; Villeval, J. L. JAK2V617F Expression in Murine Hematopoietic Cells Leads to MPD Mimicking Human PV with Secondary Myelofibrosis. *Blood* **2006**, *108*, 1652–1660.

- (13) Wernig, G.; Mercher, T.; Okabe, R.; Levine, R. L.; Lee, B. H.; Gilliland, D. G. Expression of Jak2V617F Causes a Polycythemia Vera-like Disease with Associated Myelofibrosis in a Murine Bone Marrow Transplant Model. *Blood* **2006**, *107*, 4274–4281.

- (14) Lucia, E.; Recchia, A. G.; Gentile, M.; Bossio, S.; Vigna, E.; Mazzone, C.; Madeo, A.; Morabito, L.; Gigliotti, V.; De Stefano, L.; Caruso, N.; Servillo, P.; Franzese, S.; Bisconte, M. G.; Gentile, C.; Morabito, F. Janus Kinase 2 Inhibitors in Myeloproliferative Disorders. *Expert Opin. Invest. Drugs* **2011**, *20*, 41–59 and references therein.

- (15) Thompson, J. E.; Cubbon, R. M.; Cummings, R. T.; Wicker, L. S.; Frankshun, R.; Cunningham, B. R.; Cameron, P. M.; Meinke, P. T.; Liverton, N.; Weng, Y.; DeMartino, J. A. Photochemical Preparation of a Pyridone Containing Tetracycle: A Jak Protein Kinase Inhibitor. *Bioorg. Med. Chem. Lett.* **2002**, *12*, 1219–1223.

- (16) Goulet, J. L.; Hong, X.; Sinclair, P. J.; Thompson, J. E.; Cubbon, R. M.; Cummings, R. T. Preparation of Benzimidazo[4,5-f]isoquinolines as Inhibitors of Janus Protein Tyrosine Kinases (Jak). WO 2003/011285, 2003.

- (17) Young, J. R.; Haidle, A.; Tempest, P.; Machacek, M. Preparation of Benzoimidazoisoquinolines as Inhibitors of Janus Kinases. WO 2007/145957, 2007.

- (18) Mathur, A.; Mo, J.-R.; Kraus, M.; O'Hare, E.; Sinclair, P.; Young, J.; Zhao, S.; Wang, Y.; Kopinja, J.; Qu, X.; Reilly, J.; Walker, D.; Xu, L.; Aleksandrowicz, D.; Marshall, G.; Scott, M. L.; Kohl, N. E.; Bachman, E. An Inhibitor of Janus Kinase 2 Prevents Polycythemia in Mice. *Biochem. Pharmacol.* **2009**, *78*, 382–389.

- (19) Truchon, J.-F.; Lachance, N.; Lau, C.; Leblanc, Y.; Mellon, C.; Roy, P.; Isabel, E.; Otte, R. D.; Young, J. R. Preparation of Tricyclic Compounds Useful as Inhibitors of Kinases. WO 2007/061764, 2007.

- (20) Friesen, R. W.; Ducharme, Y.; Ball, R. G.; Blouin, M.; Boulet, L.; Cote, B.; Frenette, R.; Girard, M.; Guay, D.; Huang, Z.; Jones, T. R.; Laliberte, F.; Lynch, J. J.; Mancini, J.; Martins, E.; Masson, P.; Muise, E.; Pon, D. J.; Siegel, P. K. S.; Styhler, A.; Tsou, N. N.; Turner, M. J.; Young, R. N.; Girard, Y. Optimization of a Tertiary Alcohol Series of Phosphodiesterase-4 (PDE4) Inhibitors: Structure–Activity Relationship Related to PDE4 Inhibition and Human Ether-a-go-go Related Gene Potassium Channel Binding Affinity. *J. Med. Chem.* **2003**, *46*, 2413–2426.

- (21) Miyaura, N.; Suzuki, A. Palladium-Catalyzed Cross-Coupling Reactions of Organoboron Compounds. *Chem. Rev.* **1995**, *95*, 2457–2483.

- (22) Littke, A. F.; Fu, G. C. A Convenient and General Method for Pd-Catalyzed Suzuki Cross-Couplings of Aryl Chlorides and Arylboronic Acids. *Angew. Chem., Int. Ed.* **1998**, *37*, 3387–3388.

- (23) Tschäen, D. M.; Desmond, R.; King, A. O.; Fortin, M. C.; Pipik, B.; King, S.; Verhoeven, T. R. An Improved Procedure for Aromatic Cyanation. *Synth. Commun.* **1994**, *24*, 887–890.

- (24) Nguyen, C. H.; Bisagni, E. Synthesis of Tricyclic Analogs of Ellipticines: 4-Methyl-5H-pyrido[4,3-b]indoles ( $\gamma$ -Carbolines) with Various Substituents at Their Apexes 1, 5 and 8. *Tetrahedron* **1987**, *43*, 527–535.

- (25) Muci, A. R.; Buchwald, S. L. Practical Palladium Catalysts for C–N and C–O Bond Formation. *Top. Curr. Chem.* **2002**, *219*, 131–209.

- (26) Hartwig, J. F. Carbon–Heteroatom Bond Formation Catalyzed by Organometallic Complexes. *Nature* **2008**, *455*, 314–322.

- (27) Liu, G.; Cogan, D. A.; Owens, T. D.; Tang, T. P.; Ellman, J. A. Synthesis of Enantiomerically Pure *N-tert*-Butanesulfinyl Imines

(*tert*-Butanesulfinimines) by the Direct Condensation of *tert*-Butanesulfinamide with Aldehydes and Ketones. *J. Org. Chem.* **1999**, *64*, 1278–1284.

(28) Robak, M. T.; Herbage, M. A.; Ellman, J. A. Synthesis and Applications of *tert*-Butanesulfinamide. *Chem. Rev.* **2010**, *110*, 3600–3740.

(29) Prakash, G. K. S.; Mandal, M.; Olah, G. A. Asymmetric Synthesis of Trifluoromethylated Allylic Amines Using  $\alpha,\beta$ -Unsaturated *N-tert*-Butanesulfinimines. *Org. Lett.* **2001**, *3*, 2847–2850.

(30) Smith, D. A.; Jones, B. C.; Walker, D. K. Design of Drugs Involving the Concepts and Theories of Drug Metabolism and Pharmacokinetics. *Med. Res. Rev.* **1996**, *16*, 243–266.

(31) Manoury, P. M.; Binet, J. L.; Rousseau, J.; Lefevre-Borg, F. M.; Cavero, I. G. Synthesis of a Series of Compounds Related to Betaxolol, a New  $\beta_1$ -Adrenoceptor Antagonist with a Pharmacological and Pharmacokinetic Profile Optimized for the Treatment of Chronic Cardiovascular Diseases. *J. Med. Chem.* **1987**, *30*, 1003–1011.

(32) Schoemaker, H.; Hicks, P.; Langer, S. Calcium Channel Receptor Binding Studies for Diltiazem and Its Major Metabolites: Functional Correlation to Inhibition of Portal Vein Myogenic Activity. *J. Cardiovasc. Pharmacol.* **1987**, *9*, 173–180.

(33) Priest, B. T.; Garcia, M. L.; Middleton, R. E.; Brochu, R. M.; Clark, S.; Dai, G.; Dick, I. E.; Felix, J. P.; Liu, C. J.; Reiser, B. S.; Schmalhofer, W. A.; Shao, P. P.; Tang, Y. S.; Chou, M. Z.; Kohler, M. G.; Smith, M. M.; Warren, V. A.; Williams, B. S.; Cohen, C. J.; Martin, W. J.; Meinke, P. T.; Parsons, W. H.; Wafford, K. A.; Kaczorowski, G. J. A Disubstituted Succinamide Is a Potent Sodium Channel Blocker with Efficacy in a Rat Pain Model. *Biochemistry* **2004**, *43*, 9866–9876.

(34) Kraus, M.; Wang, Y.; Aleksandrowicz, D.; Bachman, E.; Szewczak, A. A.; Walker, D.; Xu, L.; Bouthillette, M.; Childers, K. M.; Dolinski, B.; Haidle, A. M.; Kopinja, J.; Lee, L.; Lim, J.; Little, K. D.; Ma, Y.; Mathur, A.; Mo, J.-R.; O'Hare, E.; Otte, R.; Rosenstein, C.; Taoka, B. M.; Wang, W.; Hong, Y.; Zabierek, A. A.; Zhang, W.; Zhao, S.; Zhu, J.; Young, J.; Marshall, C. G. Unpublished results.

(35) Young, J. R.; Lim, J.; Machacek, M. R.; Taoka, B. M.; Otte, R. D. Preparation of *5H*-Pyrido[4,3-*b*]indole Derivatives as Janus Kinases Inhibitors. WO 2009/075830, 2009.

(36) Otwinowski, Z.; Minor, W. Processing of X-ray Diffraction Data Collected in Oscillation Mode. *Methods Enzymol.* **1997**, *276*, 307–326.

(37) McCoy, A. J.; Grosse-Kunstleve, R. W.; Adams, P. D.; Winn, M. D.; Storoni, L. C.; Read, R. J. Phaser Crystallographic Software. *J. Appl. Crystallogr.* **2007**, *40*, 658–674.

(38) Emsley, P.; Lohkamp, B.; Scott, W. G.; Cowtan, K. Features and Development of Coot. *Acta Crystallogr.* **2010**, *D66*, 486–501.

(39) Murshudov, G. N.; Vagin, A. A.; Dodson, E. J. Refinement of Macromolecular Structures by the Maximum-Likelihood Method. *Acta Crystallogr.* **1997**, *D53*, 240–255.